Advanced Control Strategies for the Robotic Hand

A THESIS

SUBMITTED TO THE FACULTY OF

THE UNIVERSITY OF MINNESOTA

BY

Ibrahim Baz Khallouf

IN PARTIAL FULFILLMENT OF THE REQUIERMENTS

FOR THE DEGREE OF

MASTER OF SCIENCE

Prof. Desineni Subbaram Naidu

December, 2017

Abstract

The research in this master's thesis presents a new state-space representation of the nonlinear dynamics of two-link (thumb) and three-link (index) fingers of a robotic hand and an effective online solution of finite-time, nonlinear, closed-loop optimal control regulator and tracking problems using the state-dependent Riccati equations (SDRE). The technique involves the use of the solution of the algebraic Riccati equation for the infinite-time case (hence the technique is approximate) and the change of variables that converts a state-dependent, nonlinear, differential Riccati equation (SD-DRE) to a linear differential Lyapunov equation (DLE) which can be solved in closed form. The approximate technique is demonstrated by software simulation and hardware experimentation for the two-link and three-link fingers of the robotic hand.

Contents

List of Tables

List of Figures

Chapter 1

Introduction

1.1 Background

Scientists and researchers have shown significant interest in the past few decades in the robotic hand due to the variety of its applications for prosthetic hand and robotic surgery in the medical and biomedical fields [10, 29], operations in chemical and nuclear hazardous environments [14, 5], space station building [3], and the industrial field [26].

Numerous researche studies have been conducted on the robotic hand in order to achieve an optimal model that can imitate and simulate the motions of a healthy hand. Starting from measuring and predicating contraction and relaxation level of flex-or and extensors muscles using neural networks, along with developing a new controller to control impedance parameters such as the moment of inertia, joint stiffness and viscosity of a skeletal muscle model for a robotic/prosthetic hand. Also, control techniques have been developed for the robotic/prosthetic hand to provide the desired torque and eliminate the closed-loop error to achieve the desired angle

using linear hard or soft control strategies such as PID controller, optimal control, fuzzy logic, adaptive control, sliding mode control, artificial neural networks and genetic algorithms. A position tracking and velocity control law for a six-DOF cable-driven parallel manipulator were derived in addition to an analytical solution for the optimal controller using a computationally efficient model-based predictive control scheme. A sliding mode controller was interceded for a two-link finger along with multiple crossover GA estimation of the unknown parameters of the dynamic. An online finite-horizon optimal tracking technique was developed using the state dependent Riccati equation for two-link finger [24, 2, 19].

1.2 Problem Statement

In this research, we address the problem of finite-horizon nonlinear optimal tracking control system for a robotic hand. We aim to maintain the nonlinear variables of the hand dynamic without using any linearization techniques in order to achieve an optimal control response. State space models of the nonlinear dynamics of two-link and three-link fingers are derived considering the forward kinematics and Lagrangian equation of the hand motion in order to apply a nonlinear closed-loop optimal control technique. An online finite-time nonlinear optimal tracking controller is implemented based on the state dependent Reccati equation (SDRE) that converts a nonlinear differential Riccati equation to a linear differential Lyapunov equation and solves it forward in time. Simulation results of tracking nonlinear trajectories of thumb and index fingertips with a minimum range of tracking error are illustrated and discussed. Experiment implementations and demonstrations using the SDRE technique is carried out for two-link and three-link fingers.

1.3 Chapters Review

This dissertation is composed of **five** chapters covering the following topics:

1. **Chapter 1** provides an introduction, research goals and contributions of the work.

2. **Chapter 2** presents an overview of finite-time linear optimal regulation and tracking problems and introduces the finite-horizon deferential state dependent Riccati equation (SDRE) technique.

3. **Chapter 3** expounds the dynamic of the robotic hand via forward kinematics and Lagrangian approach and presents the derivation of state space model of two-link and three-link fingers.

4. **Chapter 4** illustrates the results of simulations and embedded real-time experiments of two-link (thumb) and three-link (index) fingers using the state dependent Riccati equation (SDRE) technique.

5. **Chapter 5** presents the discussion and conclusion of simulation and embedded real-time experiment results of two-link (thumb) and three-link (index)fingers and future work.

Chapter 2

Advanced Nonlinear Control System Techniques

Due to advanced modeling techniques and modern mathematical software, engineers have become more capable of achieving precise mathematical models that describe the dynamic behavior of various systems such as biomedical systems, aerospace and automotive systems, robotics and many others. The vast majority of these systems are nonlinear [4], and they contain differential terms, yet engineers tend to linearize these systems in order to eliminate the nonlinear terms and apply linear control theories [9]. Therefore, an urgent need for nonlinear control systems has increased over the last decades, which has led to develop nonlinear control system techniques that maintain the nonlinearity features of nonlinear dynamics. The state Dependent Riccati equation (SDRE) has evolved a solution that is used significantly for the purpose of designing nonlinear control systems [6].

2.1 Finite-Time Linear Quadratic Regulator System: Overview

Consider the time-varying linear system [21]

$$\begin{aligned} \dot{\mathbf{x}}(t) &= \mathbf{A}(t)\mathbf{x}(t) + \mathbf{B}(t)\mathbf{u}(t) \\ \mathbf{y}(t) &= \mathbf{C}(t)\mathbf{x}(t) \end{aligned} \tag{2.1.1}$$

The terminal cost function is

$$\begin{aligned} J &= \frac{1}{2}\mathbf{x}'(t_f)\mathbf{F}(t_f)\mathbf{x}(t_f) \\ &\quad + \frac{1}{2}\int_{t_0}^{t_f} \left[\mathbf{x}'(t)\mathbf{Q}(t)\mathbf{x}(t) + \mathbf{u}'(t)\mathbf{R}(t)\mathbf{u}(t)\right] dt \end{aligned} \tag{2.1.2}$$

where $\mathbf{A}(t)$ is nxn state matrix, $\mathbf{B}(t)$ is nxr control matrix, $\mathbf{C}(t)$ is mxn output matrix, the control signal $\mathbf{u}(t)$ is unconstrained, t_f is specified, $\mathbf{x}(t_f)$ is unknown, the terminal cost weighted matrix $\mathbf{F}(t_f)$ and the state weighted matrix $\mathbf{Q}(t)$ are nxn symmetric, positive semidefinite matrices, and the control weighted matrix $\mathbf{R}(t)$ is rxr symmetric, positive definite.

The optimal control law is

$$\boxed{\mathbf{u}^*(t) = -\mathbf{R}^{-1}(t)\mathbf{B}'(t)\mathbf{P}(t)\mathbf{x}^*(t) = -\mathbf{K}(t)\mathbf{x}^*(t)} \tag{2.1.3}$$

where Kalman gain $\mathbf{K}(t) = \mathbf{R}^{-1}(t)\mathbf{B}'(t)\mathbf{P}(t)$ and Riccati coefficient matrix $\mathbf{P}(t)$, the nxn symmetric, *positive definite* matrix (for all $t \in [t_0, t_f]$), are the solution of the matrix differential Riccati equation (DRE)

$$\boxed{\dot{\mathbf{P}}(t) = -\mathbf{P}(t)\mathbf{A}(t) - \mathbf{A}'(t)\mathbf{P}(t) - \mathbf{Q}(t) + \mathbf{P}(t)\mathbf{B}(t)\mathbf{R}^{-1}(t)\mathbf{B}'(t)\mathbf{P}(t)} \tag{2.1.4}$$

with the final condition

$$\boxed{\mathbf{P}(t = t_f) = \mathbf{F}(t_f)} \tag{2.1.5}$$

The optimal state can be obtained as

$$\boxed{\dot{\mathbf{x}}^*(t) = \left[\mathbf{A}(t) - \mathbf{B}(t)\mathbf{R}^{-1}(t)\mathbf{B}'(t)\mathbf{P}(t)\right]\mathbf{x}^*(t)} \tag{2.1.6}$$

The optimal performance index is

$$\boxed{J^* = \frac{1}{2}\mathbf{x}^{*\prime}(t)\mathbf{P}(t)\mathbf{x}^*(t)} \tag{2.1.7}$$

The optimal control $\mathbf{u}^*(t)$, given by (2.1.3), is *linear* in the optimal state $\mathbf{x}^*(t)$. Using the Kalman gain, DRE equation (2.1.4) becomes

$$\boxed{-\dot{\mathbf{P}}(t) = \mathbf{P}(t)\left[\mathbf{A}(t) - \mathbf{B}(t)\mathbf{K}(t)\right] + \left[\mathbf{A}(t) - \mathbf{B}(t)\mathbf{K}(t)\right]'\mathbf{P}(t) + \mathbf{K}'(t)\mathbf{R}(t)\mathbf{K}(t) + \mathbf{Q}(t)} \tag{2.1.8}$$

The finite-time linear optimal control regulator procedure is summarized in Table 2.1.

2.1.1 Salient Features

1. *Riccati Coefficient:* The Riccati matrix $\mathbf{P}(t)$ is a time-dependent matrix that only counts on the system matrices $\mathbf{A}(t)$ and $\mathbf{B}(t)$, the performance index matrices $\mathbf{Q}(t)$, $\mathbf{R}(t)$ and $\mathbf{F}(t_f)$, and the final time t_f, but does not count on the initial state $\mathbf{x}(t_0)$.

2. *Optimal Control:* The optimal control $\mathbf{u}^*(t)$ (2.1.3) is minimum or maximum if the control weighted matrix $\mathbf{R}(t)$ is *positive definite* or *negative definite*, respectively.

3. *Definiteness of the Riccati Matrix* $\mathbf{P}(t)$*:* Since the terminal cost weighted matrix $\mathbf{F}(t_f)$ is positive semidefinite, and $\mathbf{P}(t_f) = \mathbf{F}(t_f)$, then we can state that $\mathbf{P}(t_f)$ is *positive semidefinite*.

4. *Computation of Matrix DRE:* DRE matrix (2.1.4) is supposed to be solved backward by integrating the DRE matrix starting from its final condition but

Table 2.1: Procedure Summary of Finite-Time Linear Quadratic Regulator System: Time-Varying Case

The Problem Statement	
Given the linear system $\dot{\mathbf{x}}(t) = \mathbf{A}(t)\mathbf{x}(t) + \mathbf{B}(t)\mathbf{u}(t)$, the terminal cost function $J = \frac{1}{2}\mathbf{x}'(t_f)\mathbf{F}(t_f)\mathbf{x}(t_f) + \frac{1}{2}\int_{t_0}^{t_f}\left[\mathbf{x}'(t)\mathbf{Q}(t)\mathbf{x}(t) + \mathbf{u}'(t)\mathbf{R}(t)\mathbf{u}(t)\right]dt$, with the boundary conditions $\mathbf{x}(t_0) = \mathbf{x}_0$, $\quad t_f$ is specified, and $\mathbf{x}(t_f)$ is unknown, find the optimal control input, state and performance index.	
The Problem Solution	
Step 1	Solve the matrix differential Riccati equation $\dot{\mathbf{P}}(t) = -\mathbf{P}(t)\mathbf{A}(t) - \mathbf{A}'(t)\mathbf{P}(t) - \mathbf{Q}(t) + \mathbf{P}(t)\mathbf{B}(t)\mathbf{R}^{-1}(t)\mathbf{B}'(t)\mathbf{P}(t)$ *backward* in time starting with the *final* condition $\mathbf{P}(t = t_f) = \mathbf{F}(t_f)$.
Step 2	Solve the optimal state $\mathbf{x}^*(t)$ from $\dot{\mathbf{x}}^*(t) = \left[\mathbf{A}(t) - \mathbf{B}(t)\mathbf{R}^{-1}(t)\mathbf{B}'(t)\mathbf{P}(t)\right]\mathbf{x}^*(t)$ *forward* in time starting with the *initial* condition $\mathbf{x}(t_0) = \mathbf{x}_0$.
Step 3	Obtain the optimal control $\mathbf{u}^*(t)$ as $\mathbf{u}^*(t) = -\mathbf{K}(t)\mathbf{x}^*(t)$, where $\mathbf{K}(t) = \mathbf{R}^{-1}(t)\mathbf{B}'(t)\mathbf{P}(t)$.
Step 4	Obtain the optimal performance index as $J^* = \frac{1}{2}\mathbf{x}^{*\prime}(t)\mathbf{P}(t)\mathbf{x}^*(t)$.

in some cases an analytical solution can be obtained for the nonlinear matrix the DRE.

5. *Independence of the Riccati Coefficient Matrix* $\mathbf{P}(t)$*:* Since the Riccati matrix $\mathbf{P}(t)$ is independent of the optimal state $\mathbf{x}^*(t)$, then once the plant matrices $\mathbf{A}(t)$ and $\mathbf{B}(t)$, and the weighted matrices $\mathbf{F}(t_f)$, $\mathbf{Q}(t)$, and $\mathbf{R}(t)$ are determined, we are *independently* capable of calculating Riccati matrix $\mathbf{P}(t)$. In general, we calculate the matrix $\mathbf{P}(t)$ off-line from its final condition in the *backward* direction during the interval $t \in [t_f, t_0]$ and conserve these off-line values before the optimal system starts operating in the forward direction. We then provide these stored values to the control system when it is operating *on-line* forward in time during the interval $t \in [t_0, t_f]$.

6. *Controllability:* Since the system is finite-time, the contribution of the uncontrollable and unstable states to the performance index function is a *finite* quantity only. Therefore, controllability condition is not required in this case.

2.2 Finite-Time Linear Quadratic Tracking System: Overview

Consider the linear observable system in Figure 2.1 [21]

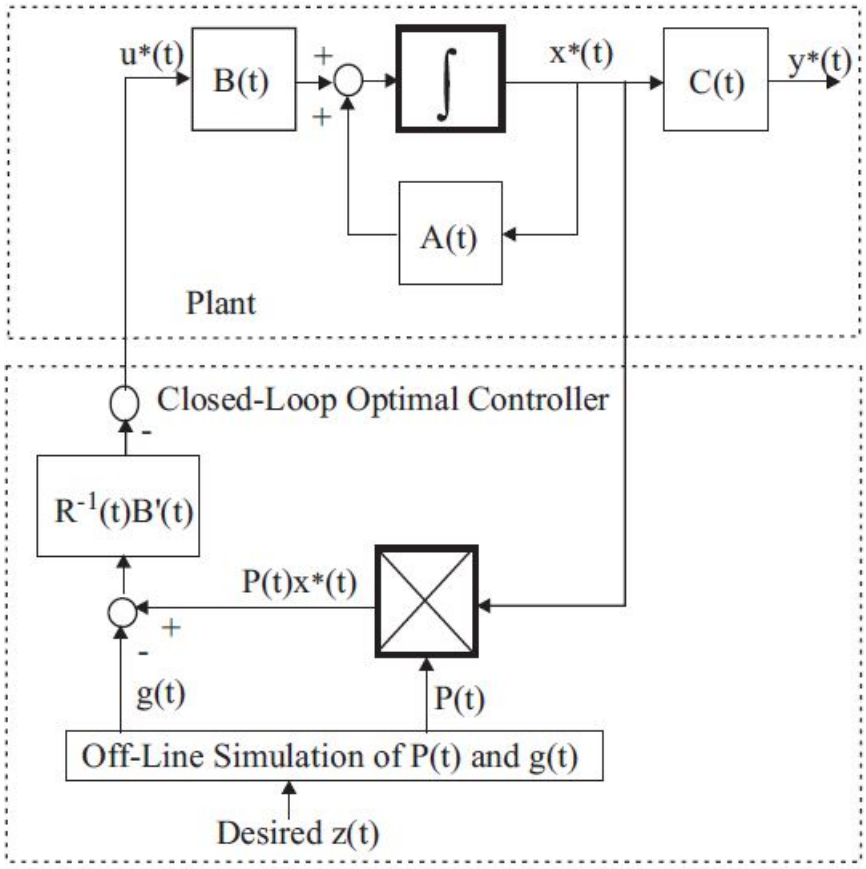

Figure 2.1: Linear Quadratic Closed-Loop Optimal Tracking System (LQT) [21]

$$\begin{aligned} \dot{\mathbf{x}}(t) &= \mathbf{A}(t)\mathbf{x}(t) + \mathbf{B}(t)\mathbf{u}(t) \\ \mathbf{y}(t) &= \mathbf{C}(t)\mathbf{x}(t) \end{aligned} \tag{2.2.1}$$

The performance index

$$J = \frac{1}{2}\mathbf{e}'(t_f)\mathbf{F}(t_f)\mathbf{e}(t_f) + \frac{1}{2}\int_{t_0}^{t_f} \left[\mathbf{e}'(t)\mathbf{Q}(t)\mathbf{e}(t) + \mathbf{u}'(t)\mathbf{R}(t)\mathbf{u}(t)\right] dt \tag{2.2.2}$$

where $\mathbf{z}(t)$ is the desired output, and the error is $\mathbf{e}(t) = \mathbf{z}(t) - \mathbf{y}(t)$.

The optimal control $\mathbf{u}^*(t)$ is

$$\begin{aligned} \mathbf{u}^*(t) &= -\mathbf{R}^{-1}(t)\mathbf{B}'(t)\left[\mathbf{P}(t)\mathbf{x}^*(t) - \mathbf{g}(t)\right] \\ &= -\mathbf{K}(t)\mathbf{x}^*(t) + \mathbf{R}^{-1}(t)\mathbf{B}'(t)\mathbf{g}(t) \end{aligned} \tag{2.2.3}$$

where Riccati coefficient matrix $\mathbf{P}(t)$, the nxn symmetric positive definite, is the solution of the nonlinear matrix differential Riccati equation (DRE)

$$\dot{\mathbf{P}}(t) = -\mathbf{P}(t)\mathbf{A}(t) - \mathbf{A}'(t)\mathbf{P}(t) + \mathbf{P}(t)\mathbf{E}(t)\mathbf{P}(t) - \mathbf{V}(t) \tag{2.2.4}$$

the final condition

$$\mathbf{P}(t_f) = \mathbf{C}'(t_f)\mathbf{F}(t_f)\mathbf{C}(t_f) \tag{2.2.5}$$

where $\mathbf{g}(t)$,nth order, is the solution of the linear nonhomogeneous vector differential equation

$$\dot{\mathbf{g}}(t) = -\left[\mathbf{A}(t) - \mathbf{E}(t)\mathbf{P}(t)\right]'\mathbf{g}(t) - \mathbf{W}(t)\mathbf{z}(t)] \tag{2.2.6}$$

with the final condition

$$\mathbf{g}(t_f) = \mathbf{C}'(t_f)\mathbf{F}(t_f)\mathbf{z}(t_f) \tag{2.2.7}$$

where the matrices $\mathbf{E}(t)$, $\mathbf{V}(t)$ and $\mathbf{W}(t)$ are

$$\begin{aligned} \mathbf{E}(t) &= \mathbf{B}(t)\mathbf{R}^{-1}(t)\mathbf{B}'(t) \\ \mathbf{V}(t) &= \mathbf{C}'(t)\mathbf{Q}(t)\mathbf{C}(t) \\ \mathbf{W}(t) &= \mathbf{C}'(t)\mathbf{Q}(t) \end{aligned} \tag{2.2.8}$$

The optimal state can be obtained from

$$\dot{\mathbf{x}}^*(t) = [\mathbf{A}(t) - \mathbf{E}(t)\mathbf{P}(t)]\,\mathbf{x}^*(t) + \mathbf{E}(t)\mathbf{g}(t)] \tag{2.2.9}$$

And the optimal performance index J^* is

$$J^*(t_0) = \frac{1}{2}\mathbf{x}^{*'}(t_0)\mathbf{P}(t_0)\mathbf{x}^*(t_0) - \mathbf{x}^{*'}(t_0)\mathbf{g}(t_0) + h(t_0) \tag{2.2.10}$$

The linear closed-loop optimal tracking control is summarized in Table 2.2 [21]

2.2.1 Salient Features of Tracking System

1. *Riccati Coefficient Matrix* $\mathbf{P}(t)$*:* The *desired output* $\mathbf{z}(t)$ has no impact upon the matrix differential Riccati equation (2.2.4) and its boundary condition (2.2.5). Therefore, once the system matrices $\mathbf{A}(t)$, $\mathbf{B}(t)$ and $\mathbf{C}(t)$, the performance index matrices $\mathbf{F}(t_f)$, $\mathbf{Q}(t)$ and $\mathbf{R}(t)$, and the final time t_f are determined, the matrix $\mathbf{P}(t)$ can be obtained.

2. *Closed Loop Eigenvalues:* The closed-loop system matrix $[\mathbf{A}(t)-\mathbf{B}(t)\mathbf{R}^{-1}(t)\mathbf{B}'(t)\mathbf{P}(t)]$ from (2.2.9) is absolutely independent of the desired output $\mathbf{z}(t)$. Therefore, we can state that the eigenvalues of the closed-loop optimal tracking system are *independent* of the desired output $\mathbf{z}(t)$ too.

3. *Tracking and Regulator Systems:* the vector $\mathbf{g}(t)$ is the main difference between the closed-loop optimal *tracking* and *regulator* systems. The desired output $\mathbf{z}(t)$ can be considered as the inducing function that generates the signal $\mathbf{g}(t)$ of the closed-loop optimal tracking system.

4. If $\mathbf{C}(t) = \mathbf{I}(t)$, then $\mathbf{V}(t) = \mathbf{Q}(t)$ in (2.2.8), then the matrix DRE (2.2.4) becomes as (2.1.4).

2.3 State Dependent Riccati Equation (SDRE)

The state dependent Riccati equation (SDRE) is a significant technique for finite-horizon nonlinear closed-loop optimal control systems that has emerged from the

Table 2.2: Summary of Linear Quadratic Tracking System

The Problem Statement	
Given the linear system $\dot{\mathbf{x}}(t) = \mathbf{A}(t)\mathbf{x}(t) + \mathbf{B}(t)\mathbf{u}(t), \quad \mathbf{y}(t) = \mathbf{C}(t)\mathbf{x}(t), \quad \mathbf{e}(t) = \mathbf{z}(t) - \mathbf{y}(t),$ the terminal cost function $J = \frac{1}{2}\mathbf{e}'(t_f)\mathbf{F}(t_f)\mathbf{e}(t_f) + \frac{1}{2}\int_{t_0}^{t_f}\left[\mathbf{e}'(t)\mathbf{Q}(t)\mathbf{e}(t) + \mathbf{u}'(t)\mathbf{R}(t)\mathbf{u}(t)\right]dt,$ with the boundary conditions $\mathbf{x}(t_0) = \mathbf{x}_0$, t_f is specified and $\mathbf{x}(t_f)$ is unknown, find the optimal control input, state and performance index.	
The Problem Solution	
Step 1	Solve the matrix differential Riccati equation (DRE) $\dot{\mathbf{P}}(t) = -\mathbf{P}(t)\mathbf{A}(t) - \mathbf{A}'(t)\mathbf{P}(t) + \mathbf{P}(t)\mathbf{E}(t)\mathbf{P}(t) - \mathbf{V}(t),$ with the final condition $\mathbf{P}(t_f) = \mathbf{C}'(t_f)\mathbf{F}(t_f)\mathbf{C}(t_f)$, and the non-homogeneous vector differential equation (DVE) $\dot{\mathbf{g}}(t) = -\left[\mathbf{A}(t) - \mathbf{E}(t)\mathbf{P}(t)\right]'\mathbf{g}(t) - \mathbf{W}(t)\mathbf{z}(t),$ with final condition $\mathbf{g}(t_f) = \mathbf{C}'(t_f)\mathbf{F}(t_f)\mathbf{z}(t_f)$ where $\mathbf{E}(t) = \mathbf{B}(t)\mathbf{R}^{-1}(t)\mathbf{B}'(t), \quad \mathbf{V}(t) = \mathbf{C}'(t)\mathbf{Q}(t)\mathbf{C}(t),$ $\mathbf{W}(t) = \mathbf{C}'(t)\mathbf{Q}(t).$
Step 2	Solve the optimal state $\mathbf{x}^*(t)$ from $\dot{\mathbf{x}}^*(t) = \left[\mathbf{A}(t) - \mathbf{E}(t)\mathbf{P}(t)\right]\mathbf{x}^*(t) + \mathbf{E}(t)\mathbf{g}(t)$ with initial condition $\mathbf{x}(t_0) = \mathbf{x}_0$.
Step 3	Obtain optimal control $\mathbf{u}^*(t)$ from $\mathbf{u}^*(t) = -\mathbf{K}(t)\mathbf{x}^*(t) + \mathbf{R}^{-1}(t)\mathbf{B}'(t)\mathbf{g}(t),$ where $\mathbf{K}(t) = \mathbf{R}^{-1}(t)\mathbf{B}'(t)\mathbf{P}(t)$.
Step 4	The optimal cost $J^*(t_0)$ is $J^*(t_0) = \frac{1}{2}\mathbf{x}^{*\prime}(t_0)\mathbf{P}(t_0)\mathbf{x}^*(t_0) - \mathbf{x}^*(t_0)\mathbf{g}(t_0) + h(t_0)$ where $h(t)$ is the solution of $\dot{h}(t) = -\frac{1}{2}\mathbf{g}'(t)\mathbf{E}(t)\mathbf{g}(t) - \frac{1}{2}\mathbf{z}'(t)\mathbf{Q}(t)\mathbf{z}(t)$ with final condition $h(t_f) = -\mathbf{z}'(t_f)\mathbf{P}(t_f)\mathbf{z}(t_f)$.

}

magnificent potential of the algebraic Riccati equation (ARE) [7, 11]. This technique is an approximate solution that depends on solving the algebraic Riccati equation (ARE) for the steady state value and applying a change of variables procedure [25], that converts a differential Riccati equation (DRE) to a linear differential Lyapunov equation (DLE) [23]. Then the procedure evaluates the coefficients of the resulting equations based on the current state values at each time interval and then freezes these coefficients from current time to the next time step. The Lyapunov equation is solved in a closed form at each interval during online implementation. The use of Lyapunov-type equations in solving optimal problems is given in [30].

2.4 Finite-Horizon Regulator for Deterministic Nonlinear Systems

In this section, we introduce the solution of the finite-horizon nonlinear differential (SDRE) technique using linear differential Layapunov equation for finite-horizon nonlinear optimal regulator problem [25].

2.4.1 Problem Formulation

Consider the *nonlinear* system:

$$\dot{\mathbf{x}}(t) = \mathbf{f}(\mathbf{x}) + \mathbf{g}(\mathbf{x})\mathbf{u}(t) \tag{2.4.1}$$

$$\mathbf{y}(t) = \mathbf{h}(\mathbf{x}) \tag{2.4.2}$$

which can also be given in a state-dependent space form as

$$\dot{\mathbf{x}}(t) = \mathbf{A}(\mathbf{x})\mathbf{x}(t) + \mathbf{B}(\mathbf{x})\mathbf{u}(t) \tag{2.4.3}$$

$$\mathbf{y}(t) = \mathbf{C}(\mathbf{x})\mathbf{x}(t) \tag{2.4.4}$$

where $\mathbf{f}(\mathbf{x}) = \mathbf{A}(\mathbf{x})\mathbf{x}(t)$, $\mathbf{B}(\mathbf{x}) = \mathbf{g}(\mathbf{x})$, and $\mathbf{h}(\mathbf{x}) = \mathbf{C}(\mathbf{x})\mathbf{x}(t)$.

The cost function given by [21]

$$\mathbf{J}(\mathbf{x},\mathbf{u}) = \frac{1}{2}\mathbf{x}'(t_f)\mathbf{F}\mathbf{x}(t_f) + \frac{1}{2}\int_{t_0}^{t_f} [\mathbf{x}'(t)\mathbf{Q}(\mathbf{x})\mathbf{x}(t) + \mathbf{u}'(\mathbf{x})\mathbf{R}(\mathbf{x})\mathbf{u}(\mathbf{x})]\ dt \quad (2.4.5)$$

where the matrices $\mathbf{Q}(\mathbf{x})$ and $\mathbf{F}$ are symmetric *positive semi-definite* matrices, and $\mathbf{R}(\mathbf{x})$ is a symmetric *positive definite* matrix.

2.4.2 Solution for Finite-Horizon Regulator Problem Using Differential (SDRE)

In optimal control problems we aim to eliminate the closed-loop error by minimizing the cost function. This goal can be achieved by obtaining a state closed-loop optimal control law as the following

$$\mathbf{u}(\mathbf{x}) = -\mathbf{K}\mathbf{x}(t) = -\mathbf{R}^{-1}(\mathbf{x})\mathbf{B}'(\mathbf{x})\mathbf{P}(\mathbf{x})\mathbf{x}(t) \quad (2.4.6)$$

where $\mathbf{P}(\mathbf{x},t)$ is a symmetric, positive-definite solution of the Dependent Differential Riccati Equation (SDDRE).

$$-\dot{\mathbf{P}}(\mathbf{x}) = \mathbf{P}(\mathbf{x})\mathbf{A}(\mathbf{x}) + \mathbf{A}'(\mathbf{x})\mathbf{P}(\mathbf{x}) - \mathbf{P}(\mathbf{x})\mathbf{B}(\mathbf{x})\mathbf{R}^{-1}(\mathbf{x})\mathbf{B}'(\mathbf{x})\mathbf{P}(\mathbf{x}) + \mathbf{Q}(\mathbf{x}) \quad (2.4.7)$$

the final condition

$$\mathbf{P}(\mathbf{x},t_f) = \mathbf{F} \quad (2.4.8)$$

then the closed-loop optimal state can be obtained as

$$\dot{\mathbf{x}}(t) = [\mathbf{A}(\mathbf{x}) - \mathbf{B}(\mathbf{x})\mathbf{R}^{-1}(\mathbf{x})\mathbf{B}'(\mathbf{x})\mathbf{P}(\mathbf{x})]\mathbf{x}(t) \quad (2.4.9)$$

The state-dependent coefficients can not be obtained by integrating the differential Riccati equation (DRE) (2.4.7) backward in time from its final condition (2.4.8) due to the fact that the differential Riccati equation (DRE) is a function of $(\mathbf{x},t)$. Therefore, and in order to overcome this problem in nonlinear closed-loop optimal

control systems, an approximate analytical solution was developed [13, 23, 25] based on the algebraic Riccati equation (ARE). We start with computing the steady state value and then convert a nonlinear differential Riccati equation to a linear differential Lyapunov equation, which can be solved in closed form at every time interval.

The following procedure [18] presents the steps of the solution for the finite-horizon differential (SDRE) regulator problem:

1. Calculate the steady state value $\mathbf{P_{ss}}(\mathbf{x})$ from algebraic Riccati equation (ARE)

$$\mathbf{P_{ss}}(\mathbf{x})\mathbf{A}(\mathbf{x}) + \mathbf{A}'(\mathbf{x})\mathbf{P_{ss}}(\mathbf{x}) - \mathbf{P_{ss}}(\mathbf{x})\mathbf{B}(\mathbf{x})\mathbf{R}^{-1}(\mathbf{x})\mathbf{B}'(\mathbf{x})\mathbf{P_{ss}}(\mathbf{x}) + \mathbf{Q}(\mathbf{x}) = 0 \tag{2.4.10}$$

2. Apply a changing-of-variables procedure and assume

$$\mathbf{K}(\mathbf{x}, \mathbf{t}) = [\mathbf{P}(\mathbf{x}, \mathbf{t}) - \mathbf{P_{ss}}(\mathbf{x})]^{-1} \tag{2.4.11}$$

3. Calculate the closed-loop matrix $\mathbf{A_{cl}}(\mathbf{x})$ as

$$\mathbf{A_{cl}}(\mathbf{x}) = \mathbf{A}(\mathbf{x}) - \mathbf{B}(\mathbf{x})\mathbf{R^{-1}}\mathbf{B}'(\mathbf{x})\mathbf{P_{ss}}(\mathbf{x}) \tag{2.4.12}$$

4. Calculate $\mathbf{D}$ by solving the algebraic Lyapunov equation [12]

$$\mathbf{A_{cl}}\mathbf{D} + \mathbf{D}\mathbf{A}'_{\mathbf{cl}} - \mathbf{B}\mathbf{R}^{-1}\mathbf{B}' = 0 \tag{2.4.13}$$

5. Solve the differential Lyapunov equation

$$\dot{\mathbf{K}}(\mathbf{x}, t) = \mathbf{K}(\mathbf{x}, t)\mathbf{A}'_{\mathbf{cl}}(\mathbf{x}) + \mathbf{A_{cl}}(\mathbf{x})\mathbf{K}(\mathbf{x},t) - \mathbf{B}(\mathbf{x})\mathbf{R}^{-1}\mathbf{B}'(\mathbf{x}) \tag{2.4.14}$$

The solution of (2.4.14), as shown by [1], is given by

$$\mathbf{K}(\mathbf{x}, t) = \mathbf{e}^{\mathbf{A_{cl}}(\mathbf{t}-\mathbf{t_f})}(\mathbf{K}(\mathbf{x},t_f) - \mathbf{D})\mathbf{e}^{\mathbf{A_{cl}}'(\mathbf{t}-\mathbf{t_f})} + \mathbf{D} \tag{2.4.15}$$

6. Apply a change-of-variables procedure and obtain $\mathbf{P}(\mathbf{x}, \mathbf{t})$ as

$$\mathbf{P}(\mathbf{x}, t) = \mathbf{K}^{-1}(\mathbf{x}, t) + \mathbf{P}_{\mathbf{ss}}(t) \tag{2.4.16}$$

7. Finally, obtain the optimal control $\mathbf{u}(\mathbf{x}, t)$ as

$$\mathbf{u}(\mathbf{x}, t) = -\mathbf{R}^{-1}\mathbf{B}'(\mathbf{x})\mathbf{P}(\mathbf{x}, t)\mathbf{x}(t) \tag{2.4.17}$$

The previous steps lead us to the conclusion that this technique has a significant advantage, whereas it can be implemented online for real-time applications and solved forward in time instead of backward. Also, we should note that, differential Lyapunov equation (DLE) is obtained by solving the algebraic Riccati equation for the steady state value $\mathbf{P}_{\mathbf{ss}}(\mathbf{x})$ and the algebraic Lyapunov equation (ALE).

The SDRE technique can be applied to finite-horizon linear systems but then $\mathbf{K}(\mathbf{x}, t) = [\mathbf{P}(\mathbf{x}, t) - \mathbf{P}_{\mathbf{ss}}(\mathbf{x})]^{-1}$ becomes singular. In order to overcome this issue, we solve (ARE) for *the negative definite* value instead of *the positive definite*. In this case, we can assure that $[\mathbf{P}(\mathbf{x}, t) - \mathbf{P}_{\mathbf{ss}}(\mathbf{x})]$ is *positive definite* and the inverse is existed. In order to obtain the *the positive definite* solution of the ARE, we need to multiply the matrix $\mathbf{A}(\mathbf{x})$ with (-1) and calculate *the negative definite* value of $\mathbf{P}_{\mathbf{ss}}(\mathbf{x})$ [25].

Note : This procedure for finite-time linear systems can be applied to finite-time nonlinear systems also.

2.5 Finite-Horizon Tracking for Deterministic Nonlinear Systems

2.5.1 Problem Formulation

Consider the given nonlinear state-dependent system (2.4.4) and (2.4.3) and $\mathbf{z}(t)$ is the *desired* output or trajectory.

The goal is to eliminate the closed-loop error by minimizing the given cost function

$$\mathbf{J}(\mathbf{x},\mathbf{u}) = \frac{1}{2}\mathbf{e}'(t_f)\mathbf{F}\mathbf{e}(t_f) + \frac{1}{2}\int_{t_0}^{t_f} \left[\mathbf{e}'(t)\mathbf{Q}(\mathbf{x})\mathbf{e}(t) + \mathbf{u}'(\mathbf{x})\mathbf{R}(\mathbf{x})\mathbf{u}(\mathbf{x})\right]\, dt \qquad (2.5.1)$$

where the closed-loop error $\mathbf{e}(t) = \mathbf{z}(t) - \mathbf{y}(t)$.

2.5.2 Solution for Finite-Horizon Tracking problem using Differential (SDRE) and (VDE)

The optimal closed-loop control input is given as

$$\mathbf{u}(\mathbf{x}) = -\mathbf{R}^{-1}\mathbf{B}'(\mathbf{x})[\mathbf{P}(\mathbf{x})\mathbf{x} - \mathbf{g}(\mathbf{x})] \qquad (2.5.2)$$

where $\mathbf{P}(\mathbf{x})$, symmetric and positive-definite, is the solution of the differential (SDRE) that is given by

$$-\dot{\mathbf{P}}(\mathbf{x}) = \mathbf{P}(\mathbf{x})\mathbf{A}(\mathbf{x}) + \mathbf{A}'(\mathbf{x})\mathbf{P}(\mathbf{x}) - \mathbf{P}(\mathbf{x})\mathbf{B}(\mathbf{x})\mathbf{R}^{-1}\mathbf{B}'(\mathbf{x})\mathbf{P}(\mathbf{x}) + \mathbf{C}'(\mathbf{x})\mathbf{Q}(\mathbf{x})\mathbf{C}(\mathbf{x}) \qquad (2.5.3)$$

the final condition

$$\mathbf{P}(\mathbf{x}, t_f) = \mathbf{C}'(t_f)\mathbf{F}\mathbf{C}(t_f) \qquad (2.5.4)$$

and $\mathbf{g}(\mathbf{x})$ is a solution of the state-dependent non-homogeneous vector differential equation (VDE) which has the form

$$\dot{\mathbf{g}}(\mathbf{x}) = -[\mathbf{A}(\mathbf{x}) - \mathbf{B}(\mathbf{x})\mathbf{R}^{-1}(\mathbf{x})\mathbf{B}'(\mathbf{x})\mathbf{P}(\mathbf{x})]'\mathbf{g}(\mathbf{x}) - \mathbf{C}'(\mathbf{x})\mathbf{Q}(\mathbf{x})\mathbf{z}(\mathbf{x}) \qquad (2.5.5)$$

with the final condition

$$\mathbf{g}(\mathbf{x}, t_f) = \mathbf{C}'(t_f)\mathbf{F}\mathbf{z}(t_f) \qquad (2.5.6)$$

The optimal state law of the nonlinear closed-loop optimal tracking state-dependent

system can be obtained as

$$\dot{\mathbf{x}}(t) = [\mathbf{A}(\mathbf{x}) - \mathbf{B}(\mathbf{x})\mathbf{R}^{-1}(\mathbf{x})\mathbf{B}'(\mathbf{x})\mathbf{P}(\mathbf{x})]\mathbf{x}(t) + \mathbf{B}(\mathbf{x})\mathbf{R}^{-1}(\mathbf{x})\mathbf{B}'(\mathbf{x})\mathbf{g}(\mathbf{x}) \quad (2.5.7)$$

Similarly, an approximate analytical solution was developed based on the algebraic Riccati equation (ARE) to solve the differential Riccati equation (SDRE). The following procedure [18] presents the steps of the solution for the finite-horizon differential (SDRE) tracking problem:

1. Follow the steps (1-6) to Solve for $\mathbf{P}(\mathbf{x}, \mathbf{t})$ similar to the differential (SDRE) regulator problem

2. Calculate the steady state value $\mathbf{g_{ss}}(\mathbf{x})$ from the equation

$$\mathbf{g_{ss}}(\mathbf{x}) = [\mathbf{A}(\mathbf{x}) - \mathbf{B}(\mathbf{x})\mathbf{R}^{-1}(\mathbf{x})\mathbf{B}'(\mathbf{x})\mathbf{P_{ss}}(\mathbf{x})]'^{-1}\mathbf{C}'(\mathbf{x})\mathbf{Q}(\mathbf{x})\mathbf{z}(\mathbf{x}) \quad (2.5.8)$$

3. Apply a change-of-variables procedure and assume

$$\mathbf{K_g}(\mathbf{x}, t) = [\mathbf{g}(\mathbf{x}, t) - \mathbf{g_{ss}}(\mathbf{x})] \quad (2.5.9)$$

4. Solve the differential equation

$$\mathbf{K_g}(\mathbf{x}, t) = \mathbf{e}^{-(\mathbf{A}-\mathbf{BR}^{-1}\mathbf{B}'\mathbf{P})'(\mathbf{t}-\mathbf{t_f})}[\mathbf{g}(\mathbf{x}, t_f) - \mathbf{g_{ss}}(\mathbf{x})] \quad (2.5.10)$$

5. Apply a changing-of-variables procedure and obtain $\mathbf{g}(\mathbf{x}, t)$

$$\mathbf{g}(\mathbf{x}, t) = \mathbf{K_g}(\mathbf{x}, t) + \mathbf{g_{ss}}(\mathbf{x}) \quad (2.5.11)$$

6. Finally, obtain the optimal control input $\mathbf{u}(\mathbf{x}, t)$ as

$$\mathbf{u}(\mathbf{x}, t) = -\mathbf{R}^{-1}(\mathbf{x})\mathbf{B}'(\mathbf{x})[\mathbf{P}(\mathbf{x}, t)\mathbf{x}(t) - \mathbf{g}(\mathbf{x}, t)] \quad (2.5.12)$$

Chapter 3

Modeling and Dynamics of The Robotic Hand

3.1 Introduction

The most important requirement of designing a control system is to obtain the mathematical model that describes the dynamic of that system. Moreover, for the purpose of designing an optimal control system, the dynamic has to be rewritten in state space model. In this chapter, nonlinear state space equations of two-link and three-link fingers are derived based on the dynamic of hand motion via the Lagrangian approach considering the forward kinematics equations of a serial n-link manipulator using kinetic energy and potential energy [15, 17, 28, 27, 8, 22].

3.2 Nonlinear State Space Model

3.2.1 Two-Link Finger (Thumb)

From forward kinematics [15, 17, 28], the thumb fingertip coordinates (X^t,Y^t) (t) are obtained as

$$X^t = L_1^t cos(q_1^t) + L_2^t cos(q_1^t + q_2^t) \quad (3.2.1)$$

$$Y^t = L_1^t sin(q_1^t) + L_2^t sin(q_1^t + q_2^t) \quad (3.2.2)$$

The corresponding linear velocities ($\dot{X}^t$,$\dot{Y}^t$) of the thumb fingertip are given by

$$\begin{bmatrix} \dot{X}^t \\ \dot{Y}^t \end{bmatrix} = \begin{bmatrix} -L_1^t sin(q_1^t) - L_2^t sin(q_1^t + q_2^t) & -L_2^t sin(q_1^t + q_2^t) \\ L_1^t cos(q_1^t) + L_2^t cos(q_1^t + q_2^t) & L_2^t cos(q_1^t + q_2^t) \end{bmatrix} \begin{bmatrix} \dot{q}_1^t \\ \dot{q}_2^t \end{bmatrix}$$

or the matrix form

$$\dot{\mathbf{P}}^{\mathbf{t}} = \mathbf{J}^{\mathbf{t}} \dot{\mathbf{q}}^{\mathbf{t}} \tag{3.2.3}$$

where the matrices $\dot{\mathbf{P}}^{\mathbf{t}}$, $\dot{\mathbf{q}}^{\mathbf{t}}$, and $\mathbf{J}^{\mathbf{t}}$ are

$$\dot{\mathbf{P}}^{\mathbf{t}} = \begin{bmatrix} \dot{X}^t \\ \dot{Y}^t \end{bmatrix}; \dot{\mathbf{q}}^{\mathbf{t}} = \begin{bmatrix} \dot{q}_1^t \\ \dot{q}_2^t \end{bmatrix}; \tag{3.2.4}$$

$$\mathbf{J}^{\mathbf{t}} = \begin{bmatrix} -L_1^t sin(q_1^t) - L_2^t sin(q_1^t + q_2^t) & -L_2^t sin(q_1^t + q_2^t) \\ L_1^t cos(q_1^t) + L_2^t cos(q_1^t + q_2^t) & L_2^t cos(q_1^t + q_2^t) \end{bmatrix} \tag{3.2.5}$$

where $\mathbf{J}^{\mathbf{t}}$ is *Jacobian* matrix of the thumb. The angular velocities $\dot{q}_1^t$ and $\dot{q}_2^t$ can be obtained from (3.2.51) as

$$\dot{\mathbf{q}}^{\mathbf{t}} = \mathbf{J}^{\mathbf{t}^{-1}} \dot{\mathbf{P}}^{\mathbf{t}} \tag{3.2.6}$$

The angular accelerations $\ddot{q}_1^t$ and $\ddot{q}_2^t$ are obtained as

$$\ddot{\mathbf{q}}^{\mathbf{t}} = \mathbf{J}^{\mathbf{t}^{-1}} \left(\ddot{\mathbf{P}}^{\mathbf{t}} - \frac{d\mathbf{J}^{\mathbf{t}}}{d\mathbf{t}} \dot{\mathbf{q}}^{\mathbf{t}} \right) \tag{3.2.7}$$

where the linear acceleration vector $\ddot{\mathbf{P}}^{\mathbf{t}}$ of the thumb fingertip, $\ddot{\mathbf{q}}^{\mathbf{t}}$ and $d\mathbf{J}^{\mathbf{t}}/d\mathbf{t}$ are denoted as

$$\ddot{\mathbf{P}}^{\mathbf{t}} = \begin{bmatrix} \ddot{X}^t \\ \ddot{Y}^t \end{bmatrix}, \ddot{\mathbf{q}}^{\mathbf{t}} = \begin{bmatrix} \ddot{q}_1^t \\ \ddot{q}_2^t \end{bmatrix}, \tag{3.2.8}$$

$$\frac{d\mathbf{J}^{\mathbf{t}}}{d\mathbf{t}} = \begin{bmatrix} -L_1^t cos(q_1^t)\dot{q}_1^t - L_2^t cos(q_1^t + q_2^t)\,(\dot{q}_1^t + \dot{q}_2^t) & -L_2^t cos(q_1^t + q_2^t)\,(\dot{q}_1^t + \dot{q}_2^t) \\ -L_1^t sin(q_1^t)\dot{q}_1^t - L_2^t sin(q_1^t + q_2^t)\,(\dot{q}_1^t + \dot{q}_2^t) & -L_2^t sin(q_1^t + q_2^t)\,(\dot{q}_1^t + \dot{q}_2^t) \end{bmatrix} \tag{3.2.9}$$

By neglecting viscous friction of the motor and loaded joints, the hand motion equation via Lagrangian becomes

$$\frac{d}{dt}\left(\frac{\partial \mathcal{L}}{\partial \dot{\mathbf{q}}}\right) - \frac{\partial \mathcal{L}}{\partial \mathbf{q}} \;=\; \boldsymbol{\tau} \tag{3.2.10}$$

whereas $\mathcal{L}$ Lagrangian is:

$$\mathcal{L} \;=\; T - V \tag{3.2.11}$$

where T and V represent kinetic and potential energies, respectively. $\mathbf{q}$ is the angular position vector, $\dot{\mathbf{q}}$ the angular velocity vector, and $\boldsymbol{\tau}$ is the provided torque vector.

The Lagrangian $\mathcal{L}^t$ of two-link finger can be given as [8, 22]

$$\mathcal{L}^t \;=\; T^t - V^t \tag{3.2.12}$$

where T^t and V^t are:

$$\begin{aligned} T^t &= \sum_{k=1}^{n} T_k^t = \sum_{k=1}^{n} (T_k^{t,lin} + T_k^{t,rot}) \\ &= \sum_{k=1}^{n} (\frac{1}{2} m_k^t \mathbf{v_{ck}^t}^{\,T} \mathbf{v_{ck}^t} + \frac{1}{2} \boldsymbol{\omega_{ck}^t}^{\,T} \mathbf{I_k^t} \boldsymbol{\omega_{ck}^t}) \\ &= \sum_{k=1}^{n} (\frac{1}{2} m_k^t \frac{d}{dt}\mathbf{p_{ck}^t}^{\,T} \frac{d}{dt}\mathbf{p_{ck}^t} + \frac{1}{2} \boldsymbol{\omega_{ck}^t}^{\,T} \mathbf{I_k^t} \boldsymbol{\omega_{ck}^t}) \qquad (3.2.13) \\ V^t &= \sum_{k=1}^{n} V_k^t \qquad (3.2.14) \end{aligned}$$

where $T_k^{t,lin}$ and $T_k^{t,rot}$ are the linear and rotational parts of kinetic energy, respectively; m_k^t is the mass of the link k; v_{ck}^t is the velocity vector of the center of the mass of the number link k; p_{ck}^t is the position vector of the center of the mass of the link number k; ω_{ck}^t is the angular velocity vector of the center of the mass of the link number k; I_k^t is the moment of inertia vector of the joint number$k$; V_k^t is potential energy vector of the joint number k, and n is the number of joints or links. The parameters $\mathbf{p_{ck}^t}$, $\mathbf{v_{ck}^t}$, $\boldsymbol{\omega_{ck}^t}$, $\mathbf{I_k^t}$, and V_k^t are given as

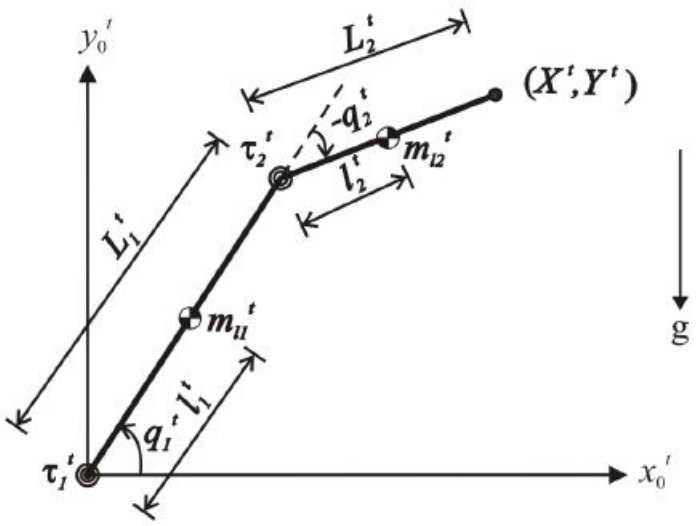

Figure 3.1: Illustration of Two-Link Manipulator (Thumb Finger) [8]

$$\mathbf{p_{c1}^t} = \begin{bmatrix} l_1^t cos(q_1^t) \\ l_1^t sin(q_1^t) \\ 0 \end{bmatrix}, \mathbf{p_{c2}^t} = \begin{bmatrix} L_1^t cos(q_1^t) + l_2^t cos(q_1^t + q_2^t) \\ L_1^t sin(q_1^t) + l_2^t sin(q_1^t + q_2^t) \\ 0 \end{bmatrix} \tag{3.2.15}$$

$$\begin{aligned} \mathbf{v_{c1}^t} &= \frac{d}{dt}\mathbf{p_{c1}^t} = \frac{d}{dt}\begin{bmatrix} l_1^t cos(q_1^t) \\ l_1^t sin(q_1^t) \\ 0 \end{bmatrix}, \\ \mathbf{v_{c2}^t} &= \frac{d}{dt}\mathbf{p_{c2}^t} = \frac{d}{dt}\begin{bmatrix} L_1^t cos(q_1^t) + l_2^t cos(q_1^t + q_2^t) \\ L_1^t sin(q_1^t) + l_2^t sin(q_1^t + q_2^t) \\ 0 \end{bmatrix} \end{aligned} \tag{3.2.16}$$

$$\boldsymbol{\omega_{c1}^t} = \frac{d}{dt}\begin{bmatrix} 0 \\ 0 \\ q_1^t \end{bmatrix} = \begin{bmatrix} 0 \\ 0 \\ \dot{q}_1^t \end{bmatrix}, \boldsymbol{\omega_{c2}^t} = \frac{d}{dt}\begin{bmatrix} 0 \\ 0 \\ q_1^t + q_2^t \end{bmatrix} = \begin{bmatrix} 0 \\ 0 \\ \dot{q}_1^t + \dot{q}_2^t \end{bmatrix} \tag{3.2.17}$$

$$\mathbf{I_1^t} = \begin{bmatrix} I_{xx1}^t & -I_{xy1}^t & -I_{xz1}^t \\ -I_{yx1}^t & I_{yy1}^t & -I_{yz1}^t \\ -I_{zx1}^t & -I_{zy1}^t & I_{zz1}^t \end{bmatrix}, \mathbf{I_2^t} = \begin{bmatrix} I_{xx2}^t & -I_{xy2}^t & -I_{xz2}^t \\ -I_{yx2}^t & I_{yy2}^t & -I_{yz2}^t \\ -I_{zx2}^t & -I_{zy2}^t & I_{zz2}^t \end{bmatrix} \tag{3.2.18}$$

$$V_1^t = m_1^t g l_1^t sin(q_1^t), V_2^t = m_2^t g L_1^t sin(q_1^t) + m_2^t g l_2^t sin(q_1^t + q_2^t) \tag{3.2.19}$$

where L_k^t is the length of the link k, l_k^t is the distance between the end of previous link and the center of mass of the link k, q_k^t is the angle of the joint number k, $I_{mnk}^t(m, n = x, y, z; k = 1, 2)$ is the inertia of the link k in x, y, and z coordinates; and g is the gravity acceleration.

The dynamic equations of the thumb can be obtained as

$$\mathbf{M(q)\ddot{q} + C(q, \dot{q}) + G(q)} = \boldsymbol{\tau} \tag{3.2.20}$$

or

$$\begin{bmatrix} M_{11}^t & M_{12}^t \\ M_{21}^t & M_{22}^t \end{bmatrix} \begin{bmatrix} \ddot{q}_1^t \\ \ddot{q}_2^t \end{bmatrix} + \begin{bmatrix} C_1^t \\ C_2^t \end{bmatrix} + \begin{bmatrix} G_1^t \\ G_2^t \end{bmatrix} = \begin{bmatrix} \tau_1^t \\ \tau_2^t \end{bmatrix} \tag{3.2.21}$$

where,

$$M_{11}^t = 2m_2^t L_1^t l_2^t cos(q_2^t) + m_1^t {l_1^t}^2 + m_2^t {L_1^t}^2 + m_2^t {l_2^t}^2 + I_{zz1}^t + I_{zz2}^t \tag{3.2.22}$$

$$M_{12}^t = m_2^t L_1^t l_2^t cos(q_2^t) + m_2^t {l_2^t}^2 + I_{zz2}^t \tag{3.2.23}$$

$$M_{21}^t = M_{12}^t \tag{3.2.24}$$

$$M_{22}^t = m_2^t {l_2^t}^2 + I_{zz2}^t \tag{3.2.25}$$

$$C_1^t = -2m_2^t L_1^t l_2^t sin(q_2^t)\dot{q}_1^t\dot{q}_2^t - m_2^t L_1^t l_2^t sin(q_2^t)\dot{q}_2^t\dot{q}_2^t \tag{3.2.26}$$

$$C_2^t = m_2^t L_1^t l_2^t sin(q_2^t)\dot{q}_1^t\dot{q}_1^t - m_2^t L_1^t l_2^t sin(q_2^t)\dot{q}_1^t\dot{q}_2^t \tag{3.2.27}$$

$$G_1^t = g(m_1^t l_1^t cos(q_1^t) + m_2^t L_1^t cos(q_1^t) + m_2^t l_2^t cos(q_1^t + q_2^t)) \tag{3.2.28}$$

$$G_2^t = g m_2^t l_2^t cos(q_1^t + q_2^t) \tag{3.2.29}$$

τ is the given torque matrix at the joints, $\mathbf{M}(\mathbf{q})$ is the inertia matrix; $\mathbf{C}(\mathbf{q}, \dot{\mathbf{q}})$ is the Coriolis/centripetal vector and $\mathbf{G}(\mathbf{q})$ is the gravity vector.

The equation (3.2.21) can be also rewritten as:

$$\begin{bmatrix} M_{11}\ddot{q_1} + M_{12}\ddot{q_2} \\ M_{21}\ddot{q_1} + M_{22}\ddot{q_2} \end{bmatrix} + \begin{bmatrix} C_1 + G_1 \\ C_2 + G_2 \end{bmatrix} = \begin{bmatrix} \tau_1 \\ \tau_2 \end{bmatrix} \tag{3.2.30}$$

Expanding the matrices in (3.2.30) we obtain

$$M_{11}\ddot{q_1} + M_{12}\ddot{q_2} + C_1 + G_1 = \tau_1 \tag{3.2.31}$$

$$M_{21}\ddot{q_1} + M_{22}\ddot{q_2} + C_2 + G_2 = \tau_2 \tag{3.2.32}$$

Now, we can derive the dynamic model of two-link finger (thumb) in state space model. From (3.2.31) we can write $\ddot{q_1}$ in terms of $\ddot{q_2}$:

$$\ddot{q_1} = -\frac{M_{12}}{M_{11}}\ddot{q_2} - \frac{1}{M_{11}}C_1 - \frac{1}{M_{11}}G_1 + \frac{1}{M_{11}}\tau_1 \tag{3.2.33}$$

Substituting $\ddot{q_1}$ in (3.2.32) we obtain

$$M_{21}(-\frac{M_{12}}{M_{11}}\ddot{q_2} - \frac{1}{M_{11}}C_1 - \frac{1}{M_{11}}G_1 + \frac{1}{M_{11}}\tau_1) + M_{22}\ddot{q_2} + C_2 + G_2 = \tau_2 \tag{3.2.34}$$

$$-\frac{M_{12}^2}{M_{11}}\ddot{q_2} - \frac{M_{12}}{M_{11}}C_1 - \frac{M_{12}}{M_{11}}G_1 + \frac{M_{12}}{M_{11}}\tau_1 + M_{22}\ddot{q_2} + C_2 + G_2 = \tau_2 \tag{3.2.35}$$

$$(M_{22} - \frac{M_{12}^2}{M_{11}})\ddot{q_2} - \frac{M_{12}}{M_{11}}C_1 - \frac{M_{12}}{M_{11}}G_1 + C_2 + G_2 = -\frac{M_{12}}{M_{11}}\tau_1 + \tau_2 \tag{3.2.36}$$

$$\begin{aligned} \ddot{q_2} \quad = \quad & \frac{M_{12}}{M_{11}M_{22} - M_{12}^2}C_1 + \frac{M_{12}}{M_{11}M_{22} - M_{12}^2}G_1 \\ & -\frac{M_{11}}{M_{11}M_{22} - M_{12}^2}C_2 - \frac{M_{11}}{M_{11}M_{22} - M_{12}^2}G_2 \\ & -\frac{M_{12}}{M_{11}M_{22} - M_{12}^2}\tau_1 + \frac{M_{11}}{M_{11}M_{22} - M_{12}^2}\tau_2 \end{aligned} \tag{3.2.37}$$

$$\begin{aligned}\ddot{q_2} &= \frac{M_{12}}{M_{11}M_{22}-M_{12}^2}\dot{q}_2C_1' + \frac{M_{12}}{M_{11}M_{22}-M_{12}^2}G_1 \\ &\quad -\frac{M_{11}}{M_{11}M_{22}-M_{12}^2}\dot{q}_1C_2' - \frac{M_{11}}{M_{11}M_{22}-M_{12}^2}G_2 \\ &\quad -\frac{M_{12}}{M_{11}M_{22}-M_{12}^2}\tau_1 + \frac{M_{11}}{M_{11}M_{22}-M_{12}^2}\tau_2 \end{aligned} \tag{3.2.38}$$

$$C_1' = -2m_2^tL_1^tl_2^tsin(q_2^t)\dot{q}_1^t - m_2^tL_1^tl_2^tsin(q_2^t)\dot{q}_2^t \tag{3.2.39}$$

$$C_2' = m_2^tL_1^tl_2^tsin(q_2^t)\dot{q}_1^t - m_2^tL_1^tl_2^tsin(q_2^t)\dot{q}_2^t \tag{3.2.40}$$

We can obtain $\ddot{q_1}$ by substituting $\ddot{q_2}$ from (3.2.37) to (3.2.33):

$$\begin{aligned}\ddot{q_1} &= -\frac{M_{12}}{M_{11}}(\frac{M_{12}}{M_{11}M_{22}-M_{12}^2}C_1 + \frac{M_{12}}{M_{11}M_{22}-M_{12}^2}G_1 \\ &\quad -\frac{M_{11}}{M_{11}M_{22}-M_{12}^2}C_2 - \frac{M_{11}}{M_{11}M_{22}-M_{12}^2}G_2 \\ &\quad -\frac{M_{12}}{M_{11}M_{22}-M_{12}^2}\tau_1 + \frac{M_{12}}{M_{11}M_{22}-M_{12}^2}\tau_2) \\ &\quad -\frac{1}{M_{11}}C_1 - \frac{1}{M_{11}}G_1 + \frac{1}{M_{11}}\tau_1 \end{aligned} \tag{3.2.41}$$

$$\begin{aligned}\ddot{q_1} &= -\frac{M_{12}^2}{M_{11}(M_{11}M_{22}-M_{12}^2)}C_1 - \frac{M_{12}^2}{M_{11}(M_{11}M_{22}-M_{12}^2)}G_1 \\ &\quad +\frac{M_{12}}{M_{11}M_{22}-M_{12}^2}C_2 + \frac{M_{12}}{M_{11}M_{22}-M_{12}^2}G_2 \\ &\quad +\frac{M_{12}^2}{M_{11}(M_{11}M_{22}-M_{12}^2)}\tau_1 + \frac{M_{12}}{M_{11}M_{22}-M_{12}^2}\tau_2 \\ &\quad -\frac{1}{M_{11}}C_1 - \frac{1}{M_{11}}G_1 + \frac{1}{M_{11}}\tau_1 \end{aligned} \tag{3.2.42}$$

$$\begin{aligned}
\ddot{q_1} &= -\frac{1}{M_{11}}(\frac{M_{12}^2 + M_{11}M_{22} - M_{12}^2}{M_{11}M_{22} - M_{12}^2})C_1 \\
&\quad -\frac{1}{M_{11}}(\frac{M_{12}^2 + M_{11}M_{22} - M_{12}^2}{M_{11}M_{22} - M_{12}^2})G_1 \\
&\quad +\frac{M_{12}}{M_{11}M_{22} - M_{12}^2}C_2 + \frac{M_{12}}{M_{11}M_{22} - M_{12}^2}G_2 \\
&\quad -\frac{1}{M_{11}}(\frac{M_{12}^2 + M_{11}M_{22} - M_{12}^2}{M_{11}M_{22} - M_{12}^2})\tau_1 \\
&\quad -\frac{M_{12}}{M_{11}M_{22} - M_{12}^2}\tau_2 \qquad (3.2.43)
\end{aligned}$$

$$\begin{aligned}
\ddot{q_1} &= -\frac{M_{22}}{M_{11}M_{22} - M_{12}^2}C_1 - \frac{M_{22}}{M_{11}M_{22} - M_{12}^2}G_1 \\
&\quad -\frac{M_{12}}{M_{11}M_{22} - M_{12}^2}C_2 - \frac{M_{12}}{M_{11}M_{22} - M_{12}^2}G_2 \\
&\quad +\frac{M_{22}}{M_{11}M_{22} - M_{12}^2}\tau_1 - \frac{M_{12}}{M_{12}M_{22} - M_{12}^2}\tau_2 \qquad (3.2.44)
\end{aligned}$$

$$\begin{aligned}
\ddot{q_1} &= -\frac{M_{22}}{M_{11}M_{22} - M_{12}^2}\dot{q_2}C_1' - \frac{M_{22}}{M_{11}M_{22} - M_{12}^2}G_1 \\
&\quad \frac{M_{12}}{M_{11}M_{22} - M_{12}^2}\dot{q_1}C_2' + \frac{M_{12}}{M_{11}M_{22} - M_{12}^2}G_2 \\
&\quad +\frac{M_{22}}{M_{11}M_{22} - M_{12}^2}\tau_1 - \frac{M_{12}}{M_{12}M_{22} - M_{12}^2}\tau_2 \qquad (3.2.45)
\end{aligned}$$

The accelerations of two-link finger are given in terms the velocities as:

$$\ddot{q_1} = M_3C_2'\dot{q_1} - M_2C_1'\dot{q_2} - M_2G_1 + M_3G_2 + M_2\tau_1 - M_3\tau_2 \qquad (3.2.46)$$

$$\ddot{q_2} = M_3C_1'\dot{q_2} - M_1C_2'\dot{q_1} + M_3G_1 - M_1G_2 - M_3\tau_1 + M_1\tau_2 \qquad (3.2.47)$$

where,

$$M_1 = \frac{M_{11}}{M_{11}M_{22} - M_{12}^2}, M_2 = \frac{M_{22}}{M_{11}M_{22} - M_{12}^2}, M_3 = \frac{M_{12}}{M_{11}M_{22} - M_{12}^2}$$

Now, taking a closer look at the inertia matrix in (3.2.21), we can clearly recognize that the dominator $(M_{11}M_{22} - M_{12}^2)$ is the determiner of the inertia matrix. Therefore, the length and mass values of the two-link finger (thumb) should be selected carefully in order to satisfy the condition $(M_{11}M_{22} - M_{12}^2 \neq 0)$ so, we can guarantee that the inertia matrix is positive definite and its inverse is exists.

The state space model of the two-link finger (thumb) of the robotic/prosthetic hand is given by:

$$\begin{bmatrix} \dot{x_1} \\ \dot{x_2} \\ \dot{x_3} \\ \dot{x_4} \end{bmatrix} = \begin{bmatrix} 0 & 1 & 0 & 0 \\ 0 & M_3C_2' & 0 & -M_2C_1' \\ 0 & 0 & 0 & 1 \\ 0 & -M_1C_2' & 0 & M_3C_1' \end{bmatrix} \begin{bmatrix} x_1 \\ x_2 \\ x_3 \\ x_4 \end{bmatrix} + \begin{bmatrix} 0 & 0 \\ M_2 & -M_3 \\ 0 & 0 \\ -M_3 & M_1 \end{bmatrix} \begin{bmatrix} u_1 \\ u_2 \end{bmatrix} \tag{3.2.48}$$

where,

$$u_1 = \tau_1 - G_1,\ u_2 = \tau_2 - G_2$$

x_1, x_3 are the angular positions q_1, q_2, and $\dot{x_1} = x_2, \dot{x_3} = x_4$ are the angular velocities $\dot{q_1}, \dot{q_2}$, and $\ddot{x_2}, \ddot{x_4}$ are the angular accelerations $\ddot{q_1}, \ddot{q_2}$, respectively.

3.2.2 Three-Link Finger (Index)

Similarly, from forward kinematics [16, 20, 31], the index fingertip coordinates (X^t,Y^t) are obtained as

$$X^i = d + L_1^i cos(q_1^i) + L_2^i cos(q_1^i + q_2^i) + L_3^i cos(q_1^i + q_2^i + q_3^i) \tag{3.2.49}$$

$$Y^i = L_1^i sin(q_1^i) + L_2^i sin(q_1^i + q_2^i) + L_3^i sin(q_1^i + q_2^i + q_3^i) \tag{3.2.50}$$

The corresponding linear velocities ($\dot{X^t}$,$\dot{Y^t}$) of the index fingertip are given by

$$\dot{\mathbf{P}}^{\mathbf{t}} = \mathbf{J}^{\mathbf{t}}\dot{\mathbf{q}}^{\mathbf{t}}. \tag{3.2.51}$$

where $\dot{\mathbf{P}}^{\mathbf{t}}$ the linear velocity vector, and $\dot{\mathbf{q}}^{\mathbf{t}}$ the angular velocity vector, and $\mathbf{J}^{\mathbf{t}}$ is

Jacobian matrix. The angular velocities $\dot{q}_1^t$, $\dot{q}_2^t$ and $\dot{q}_3^t$ are obtained as

$$\dot{\mathbf{q}}^{\mathbf{t}} \;=\; \mathbf{J}^{\mathbf{t}^{-1}}\dot{\mathbf{P}}^{\mathbf{t}}. \tag{3.2.52}$$

The angular accelerations $\dot{q}_1^t$, $\dot{q}_2^t$ and $\dot{q}_3^t$ are obtained as

$$\ddot{\mathbf{q}}^{\mathbf{t}} \;=\; \mathbf{J}^{\mathbf{t}^{-1}}\left(\ddot{\mathbf{P}}^{\mathbf{t}} - \frac{d\mathbf{J}^{\mathbf{t}}}{d\mathbf{t}}\dot{\mathbf{q}}^{\mathbf{t}}\right), \tag{3.2.53}$$

The dynamic equations of three-link finger (index) [8] can be obtained (by software Maple©) in the same form (3.2.20) as

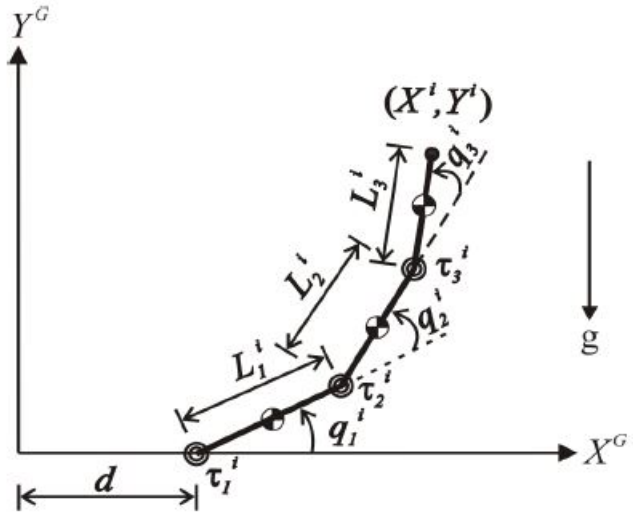

Figure 3.2: Illustration of Three-Link Manipulator (Index Finger) [8]

$$\begin{bmatrix} M_{11}^i & M_{12}^i & M_{13}^i \\ M_{21}^i & M_{22}^i & M_{23}^i \\ M_{31}^i & M_{32}^i & M_{33}^i \end{bmatrix} \begin{bmatrix} \ddot{q}_1^i \\ \ddot{q}_2^i \\ \ddot{q}_3^i \end{bmatrix} + \begin{bmatrix} C_1^i \\ C_2^i \\ C_3^i \end{bmatrix} + \begin{bmatrix} G_1^i \\ G_2^i \\ G_3^i \end{bmatrix} = \begin{bmatrix} \tau_1^i \\ \tau_2^i \\ \tau_3^i \end{bmatrix}. \tag{3.2.54}$$

where,

$$
\begin{aligned}
M^i_{11} &= 2m^i_2 L^i_1 l^i_2 sin(q^i_1) sin(q^i_1 + q^i_2) + 2m^i_2 L^i_1 l^i_2 cos(q^i_1) cos(q^i_1 + q^i_2) \\
&+2m^i_3 L^i_1 L^i_2 sin(q^i_1) sin(q^i_1 + q^i_2) \\
&+2m^i_3 L^i_1 L^i_2 cos(q^i_1) cos(q^i_1 + q^i_2) \\
&+2m^i_3 L^i_1 l^i_3 sin(q^i_1) sin(q^i_1 + q^i_2 + q^i_3) \\
&+2m^i_3 L^i_1 l^i_3 cos(q^i_1) cos(q^i_1 + q^i_2 + q^i_3) \\
&+2m^i_3 L^i_2 l^i_3 sin(q^i_1 + q^i_2) sin(q^i_1 + q^i_2 + q^i_3) \\
&+2m^i_3 L^i_2 l^i_3 cos(q^i_1 + q^i_2) cos(q^i_1 + q^i_2 + q^i_3) \\
&+m^i_1 {l^i_1}^2 + m^i_2 {L^i_1}^2 + m^i_2 {l^i_2}^2 + m^i_3 {L^i_1}^2 + m^i_3 {L^i_2}^2 + m^i_3 {l^i_3}^2 \\
&+I^i_{zz1} + I^i_{zz2} + I^i_{zz3}, \qquad (3.2.55)
\end{aligned}
$$

$$
\begin{aligned}
M^i_{12} &= m^i_2 L^i_1 l^i_2 sin(q^i_1) sin(q^i_1 + q^i_2) \\
&+m^i_2 L^i_1 l^i_2 cos(q^i_1) cos(q^i_1 + q^i_2) \\
&+2m^i_3 L^i_2 l^i_3 sin(q^i_1 + q^i_2) sin(q^i_1 + q^i_2 + q^i_3) \\
&+2m^i_3 L^i_2 l^i_3 cos(q^i_1 + q^i_2) cos(q^i_1 + q^i_2 + q^i_3) \\
&+m^i_3 L^i_1 L^i_2 sin(q^i_1) sin(q^i_1 + q^i_2) \\
&+m^i_3 L^i_1 L^i_2 cos(q^i_1) cos(q^i_1 + q^i_2) \\
&+m^i_3 L^i_1 l^i_3 sin(q^i_1) sin(q^i_1 + q^i_2 + q^i_3) \\
&+m^i_3 L^i_1 l^i_3 cos(q^i_1) cos(q^i_1 + q^i_2 + q^i_3) \\
&+m^i_2 {l^i_2}^2 + m^i_3 {L^i_2}^2 + m^i_3 {l^i_3}^2 + I^i_{zz2} + I^i_{zz3}, \qquad (3.2.56)
\end{aligned}
$$

$$
\begin{aligned}
M^i_{13} &= m^i_3 L^i_1 l^i_3 sin(q^i_1) sin(q^i_1 + q^i_2 + q^i_3) \\
&+m^i_3 L^i_1 l^i_3 cos(q^i_1) cos(q^i_1 + q^i_2 + q^i_3) \\
&+m^i_3 L^i_2 l^i_3 sin(q^i_1 + q^i_2) sin(q^i_1 + q^i_2 + q^i_3) \\
&+m^i_3 L^i_2 l^i_3 cos(q^i_1 + q^i_2) cos(q^i_1 + q^i_2 + q^i_3) \\
&+m^i_3 {l^i_3}^2 + I^i_{zz3}, \qquad (3.2.57)
\end{aligned}
$$

$$
\begin{aligned}
M^i_{21} &= M^i_{12}, && (3.2.58)\\
M^i_{22} &= 2m^i_3 L^i_2 l^i_3 sin(q^i_1+q^i_2)sin(q^i_1+q^i_2+q^i_3)\\
&\quad +2m^i_3 L^i_2 l^i_3 cos(q^i_1+q^i_2)cos(q^i_1+q^i_2+q^i_3)\\
&\quad +m^i_2 {l^i_2}^2 + m^i_3 {L^i_2}^2 + m^i_3 {l^i_3}^2 + I^i_{zz2} + I^i_{zz3}, && (3.2.59)\\
M^i_{23} &= m^i_3 L^i_2 l^i_3 sin(q^i_1+q^i_2)sin(q^i_1+q^i_2+q^i_3)\\
&\quad +m^i_3 L^i_2 l^i_3 cos(q^i_1+q^i_2)cos(q^i_1+q^i_2+q^i_3)\\
&\quad +m^i_3 {l^i_3}^2 + I^i_{zz3}, && (3.2.60)\\
M^i_{31} &= M^i_{13}, && (3.2.61)\\
M^i_{32} &= M^i_{23}, && (3.2.62)\\
M^i_{33} &= m^i_3 {l^i_3}^2 + I^i_{zz3}, && (3.2.63)
\end{aligned}
$$

$$
\begin{aligned}
G^i_1 &= g(m^i_1 l^i_1 cos(q^i_1) + m^i_2 L^i_1 cos(q^i_1) + m^i_3 L^i_1 cos(q^i_1)\\
&\quad +m^i_1 l^i_2 cos(q^i_1+q^i_2) + m^i_3 L^i_2 cos(q^i_1+q^i_2)\\
&\quad +m^i_3 l^i_3 cos(q^i_1+q^i_2+q^i_3)), && (3.2.64)\\
G^i_2 &= g(m^i_2 l^i_2 cos(q^i_1+q^i_2) + m^i_3 L^i_2 cos(q^i_1+q^i_2)\\
&\quad +m^i_3 l^i_3 cos(q^i_1+q^i_2+q^i_3)), && (3.2.65)\\
G^i_3 &= g(m^i_3 l^i_3 cos(q^i_1+q^i_2+q^i_3)). && (3.2.66)
\end{aligned}
$$

$$
\begin{aligned}
C_1^i \;=\;& (2m_2^iL_1^il_2^isin(q_1^i)cos(q_1^i+q_2^i) - 2m_2^iL_1^il_2^icos(q_1^i)sin(q_1^i+q_2^i) \\
& +2m_3^iL_1^iL_2^isin(q_1^i)cos(q_1^i+q_2^i) - 2m_3^iL_1^iL_2^icos(q_1^i)sin(q_1^i+q_2^i) \\
& +2m_3^iL_1^il_3^isin(q_1^i)cos(q_1^i+q_2^i+q_3^i) - 2m_3^iL_1^il_3^icos(q_1^i)sin(q_1^i+q_2^i+q_3^i)) \\
& \left(\frac{\partial q_1^i}{\partial t}\right)\left(\frac{\partial q_2^i}{\partial t}\right) \\
& +(2m_3^iL_1^il_3^isin(q_1^i)cos(q_1^i+q_2^i+q_3^i) - 2m_3^iL_1^il_3^icos(q_1^i)sin(q_1^i+q_2^i+q_3^i) \\
& +2m_3^iL_2^il_3^isin(q_1^i+q_2^i)cos(q_1^i+q_2^i+q_3^i) - 2m_3^iL_2^il_3^icos(q_1^i+q_2^i)sin(q_1^i+q_2^i+q_3^i)) \\
& \left(\frac{\partial q_1^i}{\partial t}\right)\left(\frac{\partial q_3^i}{\partial t}\right) \\
& +(2m_3^iL_1^il_3^isin(q_1^i)cos(q_1^i+q_2^i+q_3^i) - 2m_3^iL_1^il_3^icos(q_1^i)sin(q_1^i+q_2^i+q_3^i) \\
& +2m_3^iL_2^il_3^isin(q_1^i+q_2^i)cos(q_1^i+q_2^i+q_3^i) - 2m_3^iL_2^il_3^icos(q_1^i+q_2^i)sin(q_1^i+q_2^i+q_3^i)) \\
& \left(\frac{\partial q_2^i}{\partial t}\right)\left(\frac{\partial q_3^i}{\partial t}\right) \\
& +(m_2^iL_1^il_2^isin(q_1^i)cos(q_1^i+q_2^i) - m_2^iL_1^il_2^icos(q_1^i)sin(q_1^i+q_2^i) \\
& +m_3^iL_1^iL_2^isin(q_1^i)cos(q_1^i+q_2^i) - m_3^iL_1^iL_2^icos(q_1^i)sin(q_1^i+q_2^i) \\
& +m_3^iL_1^il_3^isin(q_1^i)cos(q_1^i+q_2^i+q_3^i) - m_3^iL_1^il_3^icos(q_1^i)sin(q_1^i+q_2^i+q_3^i)) \\
& \left(\frac{\partial q_2^i}{\partial t}\right)\left(\frac{\partial q_2^i}{\partial t}\right) \\
& +(m_3^iL_1^il_3^isin(q_1^i)cos(q_1^i+q_2^i+q_3^i) - m_3^iL_1^il_3^icos(q_1^i)sin(q_1^i+q_2^i+q_3^i) \\
& +m_3^iL_2^il_3^isin(q_1^i+q_2^i)cos(q_1^i+q_2^i+q_3^i) - m_3^iL_2^il_3^icos(q_1^i+q_2^i)sin(q_1^i+q_2^i+q_3^i)) \\
& \left(\frac{\partial q_3^i}{\partial t}\right)\left(\frac{\partial q_3^i}{\partial t}\right) \qquad (3.2.67)
\end{aligned}
$$

$$
\begin{aligned}
C_2^i \;=\;& (m_2^i L_1^i l_2^i sin(q_1^i) cos(q_1^i + q_2^i) - m_2^i L_1^i l_2^i cos(q_1^i) sin(q_1^i + q_2^i) \\
& + m_3^i L_1^i L_2^i sin(q_1^i) cos(q_1^i + q_2^i) - m_3^i L_1^i L_2^i cos(q_1^i) sin(q_1^i + q_2^i) \\
& + m_3^i L_1^i l_3^i sin(q_1^i) cos(q_1^i + q_2^i + q_3^i) - m_3^i L_1^i l_3^i cos(q_1^i) sin(q_1^i + q_2^i + q_3^i)) \\
& \left(\frac{\partial q_1^i}{\partial t}\right)\left(\frac{\partial q_2^i}{\partial t}\right) \\
& + (2m_3^i L_2^i l_3^i sin(q_1^i + q_2^i) cos(q_1^i + q_2^i + q_3^i) - 2m_3^i L_2^i l_3^i cos(q_1^i + q_2^i) sin(q_1^i + q_2^i + q_3^i)) \\
& \left(\frac{\partial q_1^i}{\partial t}\right)\left(\frac{\partial q_3^i}{\partial t}\right) \\
& + (2m_3^i L_2^i l_3^i sin(q_1^i + q_2^i) cos(q_1^i + q_2^i + q_3^i) - 2m_3^i L_2^i l_3^i cos(q_1^i + q_2^i) sin(q_1^i + q_2^i + q_3^i)) \\
& \left(\frac{\partial q_2^i}{\partial t}\right)\left(\frac{\partial q_3^i}{\partial t}\right) \\
& + (-m_2^i L_1^i l_2^i sin(q_1^i) cos(q_1^i + q_2^i) + m_2^i L_1^i l_2^i cos(q_1^i) sin(q_1^i + q_2^i) \\
& - m_3^i L_1^i L_2^i sin(q_1^i) cos(q_1^i + q_2^i) + m_3^i L_1^i L_2^i cos(q_1^i) sin(q_1^i + q_2^i) \\
& - m_3^i L_1^i l_3^i sin(q_1^i) cos(q_1^i + q_2^i + q_3^i) + m_3^i L_1^i l_3^i cos(q_1^i) sin(q_1^i + q_2^i + q_3^i)) \\
& \left(\frac{\partial q_1^i}{\partial t}\right)\left(\frac{\partial q_1^i}{\partial t}\right) \\
& + (m_3^i L_2^i l_3^i sin(q_1^i + q_2^i) cos(q_1^i + q_2^i + q_3^i) - m_3^i L_2^i l_3^i cos(q_1^i + q_2^i) sin(q_1^i + q_2^i + q_3^i)) \\
& \left(\frac{\partial q_3^i}{\partial t}\right)\left(\frac{\partial q_3^i}{\partial t}\right) \qquad (3.2.68)
\end{aligned}
$$

$$
\begin{aligned}
C_3^i &= (2m_3^iL_2^il_3^icos(q_1^i+q_2^i)sin(q_1^i+q_2^i+q_3^i) - 2m_3^iL_2^il_3^isin(q_1^i+q_2^i)cos(q_1^i+q_2^i+q_3^i)) \\
&\left(\frac{\partial q_1^i}{\partial t}\right)\left(\frac{\partial q_2^i}{\partial t}\right) \\
&+(m_3^iL_1^il_3^isin(q_1^i)cos(q_1^i+q_2^i+q_3^i) - m_3^iL_1^il_3^icos(q_1^i)sin(q_1^i+q_2^i+q_3^i) \\
&+(m_3^iL_2^il_3^isin(q_1^i+q_2^i)cos(q_1^i+q_2^i+q_3^i) - m_3^iL_2^il_3^icos(q_1^i+q_2^i)sin(q_1^i+q_2^i+q_3^i)) \\
&\left(\frac{\partial q_1^i}{\partial t}\right)\left(\frac{\partial q_3^i}{\partial t}\right) \\
&+(m_3^iL_2^il_3^isin(q_1^i+q_2^i)cos(q_1^i+q_2^i+q_3^i) - m_3^iL_2^il_3^icos(q_1^i+q_2^i)sin(q_1^i+q_2^i+q_3^i)) \\
&\left(\frac{\partial q_2^i}{\partial t}\right)\left(\frac{\partial q_3^i}{\partial t}\right) \\
&+(m_3^iL_1^il_3^icos(q_1^i)sin(q_1^i+q_2^i+q_3^i) - m_3^iL_1^il_3^isin(q_1^i)cos(q_1^i+q_2^i+q_3^i) \\
&+m_3^iL_2^il_3^icos(q_1^i+q_2^i)sin(q_1^i+q_2^i+q_3^i) - m_3^iL_2^il_3^isin(q_1^i+q_2^i)cos(q_1^i+q_2^i+q_3^i)) \\
&\left(\frac{\partial q_1^i}{\partial t}\right)\left(\frac{\partial q_1^i}{\partial t}\right) \\
&+(m_3^iL_2^il_3^icos(q_1^i+q_2^i)sin(q_1^i+q_2^i+q_3^i) - m_3^iL_2^il_3^isin(q_1^i+q_2^i)cos(q_1^i+q_2^i+q_3^i)) \\
&\left(\frac{\partial q_2^i}{\partial t}\right)\left(\frac{\partial q_2^i}{\partial t}\right) \qquad (3.2.69)
\end{aligned}
$$

The dynamic of three-link finger (index) of the robotic/prosthetic hand is given by:

$$
\begin{bmatrix} M_{11} & M_{12} & M_{13} \\ M_{21} & M_{22} & M_{23} \\ M_{31} & M_{32} & M_{33} \end{bmatrix} \begin{bmatrix} \ddot{q_1} \\ \ddot{q_2} \\ \ddot{q_3} \end{bmatrix} + \begin{bmatrix} C_1 \\ C_2 \\ C_3 \end{bmatrix} + \begin{bmatrix} G_1 \\ G_2 \\ G_3 \end{bmatrix} = \begin{bmatrix} \tau_1 \\ \tau_2 \\ \tau_3 \end{bmatrix} \qquad (3.2.70)
$$

Expanding the above matrices we obtain:

$$
M_{11}\ddot{q_1} + M_{12}\ddot{q_2} + M_{13}\ddot{q_3} + C_1 + G_1 = \tau_1 \qquad (3.2.71)
$$

$$
M_{21}\ddot{q_1} + M_{22}\ddot{q_2} + M_{23}\ddot{q_3} + C_2 + G_2 = \tau_2 \qquad (3.2.72)
$$

$$
M_{31}\ddot{q_1} + M_{32}\ddot{q_2} + M_{33}\ddot{q_3} + C_3 + G_3 = \tau_3 \qquad (3.2.73)
$$

Now, we are ready to derive the state space model of three-link finger. From (3.2.71)

we can write $\ddot{q_1}$ in terms of $\ddot{q_2}$ and $\ddot{q_3}$:

$$\ddot{q_1} = -\frac{M_{12}}{M_{11}}\ddot{q_2} - \frac{M_{13}}{M_{11}}\ddot{q_3} - \frac{1}{M_{11}}C_1 - \frac{1}{M_{11}}G_1 + \frac{1}{M_{11}}\tau_1 \tag{3.2.74}$$

Substituting $\ddot{q_1}$ from(3.2.74) in (3.2.72), we obtain $\ddot{q_2}$ in terms of $\ddot{q_3}$

$$\begin{aligned} \tau_2 &= M_{21}(-\frac{M_{12}}{M_{11}}\ddot{q_2} - \frac{M_{13}}{M_{11}}\ddot{q_3} - \frac{1}{M_{11}}C_1 - \frac{1}{M_{11}}G_1 + \frac{1}{M_{11}}\tau_1) \\ &\quad + M_{22}\ddot{q_2} + M_{23}\ddot{q_3} + C_2 + G_2 \end{aligned} \tag{3.2.75}$$

$$\begin{aligned} \tau_2 &= (\frac{M_{11}M_{22} - M_{12}^2}{M_{11}})\ddot{q_2} + (\frac{M_{11}M_{23} - M_{21}M_{13}}{M_{11}})\ddot{q_3} \\ &\quad - \frac{M_{21}}{M_{11}}C_1 - \frac{M_{21}}{M_{11}}G_1 + \frac{M_{21}}{M_{11}}\tau_1 + C_2 + G_2 \end{aligned} \tag{3.2.76}$$

$$\begin{aligned} \ddot{q_2} &= -(\frac{M_{11}M_{23} - M_{21}M_{13}}{M_{11}M_{22} - M_{12}^2})\ddot{q_3} \\ &\quad + \frac{M_{21}}{M_{11}M_{22} - M_{12}^2}C_1 + \frac{M_{21}}{M_{11}M_{22} - M_{12}^2}G_1 \\ &\quad - \frac{M_{11}}{M_{11}M_{22} - M_{12}^2}C_2 - \frac{M_{11}}{M_{11}M_{22} - M_{12}^2}G_2 \\ &\quad - \frac{M_{21}}{M_{11}M_{22} - M_{12}^2}\tau_1 + \frac{M_{11}}{M_{11}M_{22} - M_{12}^2}\tau_2 \end{aligned} \tag{3.2.77}$$

Substituting $\ddot{q_2}$ from (3.2.77) in (3.2.74), we obtain $\ddot{q_1}$ in terms of $\ddot{q_3}$

$$\begin{aligned} \ddot{q_1} &= \frac{M_{12}}{M_{11}}(\frac{M_{11}M_{23} - M_{21}M_{13}}{M_{11}M_{22} - M_{12}^2})\ddot{q_3} \\ &\quad - \frac{M_{12}^2}{M_{11}(M_{11}M_{22} - M_{12}^2)}C_1 - \frac{M_{12}^2}{M_{11}(M_{11}M_{22} - M_{12}^2)}G_1 \\ &\quad + \frac{M_{11}M_{12}}{M_{11}(M_{11}M_{22} - M_{12}^2)}C_2 + \frac{M_{11}M_{12}}{M_{11}(M_{11}M_{22} - M_{12}^2)}G_2 \\ &\quad + \frac{M_{12}^2}{M_{11}(M_{11}M_{22} - M_{12}^2)}\tau_1 - \frac{M_{11}M_{12}}{M_{11}(M_{11}M_{22} - M_{12}^2)}\tau_2 \\ &\quad - \frac{M_{13}}{M_{11}}\ddot{q_3} - \frac{1}{M_{11}}C_1 - \frac{1}{M_{11}}G_1 + \frac{1}{M_{11}}\tau_1 \end{aligned} \tag{3.2.78}$$

$$
\begin{aligned}
\ddot{q_1} &= (\frac{M_{12}M_{23}-M_{13}M_{22}}{M_{11}M_{22}-M_{12}^2})\ddot{q_3} \\
&-\frac{M_{22}}{M_{11}M_{22}-M_{12}^2}C_1-\frac{M_{22}}{M_{11}M_{22}-M_{12}^2}G_1 \\
&+\frac{M_{12}}{M_{11}M_{22}-M_{12}^2}C_2+\frac{M_{12}}{M_{11}M_{22}-M_{12}^2}G_2 \\
&+\frac{M_{22}}{M_{11}M_{22}-M_{12}^2}\tau_1-\frac{M_{12}}{M_{11}M_{22}-M_{12}^2}\tau_2
\end{aligned} \tag{3.2.79}
$$

We obtain $\ddot{q_3}$ by substituting $\ddot{q_1}$ and $\ddot{q_2}$ in (3.2.73)

$$
\begin{aligned}
\tau_3 &= M_{31}(\frac{M_{12}M_{23}-M_{13}M_{22}}{M_{11}M_{22}-M_{12}^2}\ddot{q_3} \\
&-\frac{M_{22}}{M_{11}M_{22}-M_{12}^2}C_1-\frac{M_{22}}{M_{11}M_{22}-M_{12}^2}G_1 \\
&+\frac{M_{12}}{M_{11}M_{22}-M_{12}^2}C_2+\frac{M_{12}}{M_{11}M_{22}-M_{12}^2}G_2 \\
&+\frac{M_{22}}{M_{11}M_{22}-M_{12}^2}\tau_1-\frac{M_{12}}{M_{11}M_{22}-M_{12}^2}\tau_2) \\
&+M_{32}(\frac{M_{21}M_{13}-M_{11}M_{23}}{M_{11}M_{22}-M_{12}^2}\ddot{q_3} \\
&+\frac{M_{21}}{M_{11}M_{22}-M_{12}^2}C_1+\frac{M_{21}}{M_{11}M_{22}-M_{12}^2}G_1 \\
&-\frac{M_{11}}{M_{11}M_{22}-M_{12}^2}C_2-\frac{M_{11}}{M_{11}M_{22}-M_{12}^2}G_2 \\
&-\frac{M_{21}}{M_{11}M_{22}-M_{12}^2}\tau_1+\frac{M_{11}}{M_{11}M_{22}-M_{12}^2}\tau_2) \\
&+M_{33}\ddot{q_3}+C_3+G_3
\end{aligned} \tag{3.2.80}
$$

$$
\begin{aligned}
\tau_3 &= \frac{M_{31}(M_{12}M_{23}-M_{13}M_{22})+M_{32}(M_{21}M_{13}-M_{11}M_{23})+M_{33}(M_{11}M_{22}-M_{12}^2)}{M_{11}M_{22}-M_{12}^2}\ddot{q_3} \\
&+\frac{M_{21}M_{32}-M_{22}M_{31}}{M_{11}M_{22}-M_{12}^2}C_1+\frac{M_{21}M_{32}-M_{22}M_{31}}{M_{11}M_{22}-M_{12}^2}G_1 \\
&+\frac{M_{12}M_{13}-M_{11}M_{32}}{M_{11}M_{22}-M_{12}^2}C_2+\frac{M_{12}M_{13}-M_{11}M_{32}}{M_{11}M_{22}-M_{12}^2}G_2 \\
&+\frac{M_{22}M_{31}-M_{21}M_{32}}{M_{11}M_{22}-M_{12}^2}\tau_1+\frac{M_{11}M_{32}-M_{12}M_{13}}{M_{11}M_{22}-M_{12}^2}\tau_2+C_3+G_3
\end{aligned} \tag{3.2.81}
$$

The acceleration $\ddot{q_3}$ becomes:

$$\begin{aligned}
\ddot{q_3} &= \frac{M_{22}M_{31} - M_{21}M_{32}}{M_{d3}}C_1 + \frac{M_{22}M_{31} - M_{21}M_{32}}{M_{d3}}G_1 \\
&+ \frac{M_{11}M_{32} - M_{12}M_{13}}{M_{d3}}C_2 + \frac{M_{11}M_{32} - M_{12}M_{13}}{M_{d3}}G_2 \\
&- \frac{M_{11}M_{22} - M_{12}^2}{M_{d3}}C_3 - \frac{M_{11}M_{22} - M_{12}^2}{M_{d3}}G_3 \\
&- \frac{M_{22}M_{31} - M_{21}M_{32}}{M_{d3}}\tau_1 - \frac{M_{11}M_{32} - M_{12}M_{13}}{M_{d3}}\tau_2 \\
&+ \frac{M_{11}M_{22} - M_{12}^2}{M_{d3}}\tau_3 \qquad (3.2.82)
\end{aligned}$$

where,

$$M_{d3} = M_{31}(M_{12}M_{23} - M_{13}M_{22}) + M_{32}(M_{21}M_{13} - M_{11}M_{23}) + M_{33}(M_{11}M_{22} - M_{12}^2)$$

We obtain $\ddot{q_1}$ and $\ddot{q_2}$ by substituting $\ddot{q_3}$ in (3.2.77) and (3.2.79), respectively

$$\begin{aligned}
\ddot{q_1} &= \frac{M_{23}^2 - M_{22}M_{33}}{M_{d3}}C_1 + \frac{M_{23}^2 - M_{22}M_{33}}{M_{d3}}G_1 \\
&+ \frac{M_{12}M_{33} - M_{13}M_{23}}{M_{d3}}C_2 + \frac{M_{12}M_{33} - M_{13}M_{23}}{M_{d3}}G_2 \\
&+ \frac{M_{13}M_{22} - M_{12}M_{23}}{M_{d3}}C_3 + \frac{M_{13}M_{22} - M_{12}M_{23}}{M_{d3}}G_3 \\
&- \frac{M_{23}^2 - M_{22}M_{33}}{M_{d3}}\tau_1 - \frac{M_{12}M_{33} - M_{13}M_{23}}{M_{d3}}\tau_2 \\
&- \frac{M_{13}M_{22} - M_{12}M_{23}}{M_{d3}}\tau_3 \qquad (3.2.83)
\end{aligned}$$

$$
\begin{aligned}
\ddot{q_2} &= \frac{M_{12}M_{33} - M_{13}M_{23}}{M_{d3}}C_1 + \frac{M_{12}M_{33} - M_{13}M_{23}}{M_{d3}}G_1 \\
&+ \frac{M_{13}^2 - M_{11}M_{33}}{M_{d3}}C_2 + \frac{M_{13}^2 - M_{11}M_{33}}{M_{d3}}G_2 \\
&+ \frac{M_{11}M_{23} - M_{12}M_{13}}{M_{d3}}C_3 + \frac{M_{11}M_{23} - M_{12}M_{13}}{M_{d3}}G_3 \\
&- \frac{M_{12}M_{33} - M_{13}M_{23}}{M_{d3}}\tau_1 - \frac{M_{13}^2 - M_{11}M_{33}}{M_{d3}}\tau_2 \\
&- \frac{M_{11}M_{23} - M_{12}M_{13}}{M_{d3}}\tau_3
\end{aligned} \tag{3.2.84}
$$

The third link has a $[0°, 270°]$ range of motion, while the first link has only a $[0°, 90°]$ range of motion. That leads us to the conclusion that the angular velocity is $\dot{q_1} < \dot{q_3}$ and $\dot{q_1}^2 << \dot{q_3}^2$. Therefore, the angular velocity $\dot{q_1}^2$ can be omitted in (3.2.69) and (3.2.69), since we are only interested in tracking the fingertip.

Also, based on the acquired data in [16, 20, 31] and considering the relation $\dot{q_3} = 0.7\dot{q_2}$ hence, the accelerations $\ddot{q_1}$, $\ddot{q_2}$ and $\ddot{q_3}$ can be given in terms of the velocities $\dot{q_3}$ as the following

$$
\ddot{q_1} = \dot{q_3}M_1C_1' + M_1G_1 + \dot{q_3}M_2C_2' + M_2G_2 + \dot{q_3}M_3C_3' + M_3G_3 - M_1\tau_1 - M_2\tau_2 - M_3\tau_3 \tag{3.2.85}
$$

$$
\ddot{q_2} = \dot{q_3}M_2C_1' + M_2G_1 + \dot{q_3}M_4C_2' + M_4G_2 + \dot{q_3}M_5C_3' + M_5G_3 - M_2\tau_1 - M_4\tau_2 - M_5\tau_3 \tag{3.2.86}
$$

$$
\ddot{q_3} = \dot{q_3}M_3C_1' + M_3G_1 + \dot{q_3}M_5C_2' + M_5G_2 - \dot{q_3}M_6C_3' - M_6G_3 - M_3\tau_1 - M_5\tau_2 + M_6\tau_3 \tag{3.2.87}
$$

where,

$$
M_1 = \frac{M_{23}^2 - M_{22}M_{33}}{M_{d3}}, M_2 = \frac{M_{12}M_{33} - M_{13}M_{23}}{M_{d3}}, M_3 = \frac{M_{13}M_{22} - M_{12}M_{23}}{M_{d3}}
$$

$$M_4 = \frac{M_{13}^2 - M_{11}M_{33}}{M_{d3}}, M_5 = \frac{M_{11}M_{23} - M_{12}M_{13}}{M_{d3}}, M_6 = \frac{M_{11}M_{22} - M_{12}^2}{M_{d3}}$$

The state space equation of three-link finger (index) is presented by

$$\begin{bmatrix} \dot{x_1} \\ \dot{x_2} \\ \dot{x_3} \\ \dot{x_4} \\ \dot{x_5} \\ \dot{x} \end{bmatrix} = \begin{bmatrix} 0 & 1 & 0 & 0 & 0 & 0 \\ 0 & 0 & 0 & 0 & 0 & M_1C_1' + M_2C_2' + M_3C_3' \\ 0 & 0 & 0 & 1 & 0 & 0 \\ 0 & 0 & 0 & 0 & 0 & M_2C_1' + M_4C_2' + M_5C_3' \\ 0 & 0 & 0 & 0 & 0 & 1 \\ 0 & 0 & 0 & 0 & 0 & M_3C_1' + M_5C_2' - M_6C_3' \end{bmatrix} \begin{bmatrix} x_1 \\ x_2 \\ x_3 \\ x_4 \\ x_5 \\ x_6 \end{bmatrix} + \begin{bmatrix} 0 & 0 & 0 \\ -M_1 & -M_2 & -M_3 \\ 0 & 0 & 0 \\ -M_2 & -M_4 & -M_5 \\ 0 & 0 & 0 \\ -M_3 & -M_5 & M_6 \end{bmatrix} \begin{bmatrix} u_1 \\ u_2 \\ u_3 \end{bmatrix} \tag{3.2.88}$$

where:

$$u_1 = \tau_1 - G_1,\ u_2 = \tau_2 - G_2,\ u_2 = \tau_3 - G_3$$

x_1, x_3, x_5 are the angular positions q_1, q_2, q_3, and $\dot{x_1} = x_2, \dot{x_3} = x_4, \dot{x_5} = x_6$ are the angular velocities $\dot{q_1}, \dot{q_2}, \dot{q_3}$, and $\ddot{x_2}, \ddot{x_4}, \ddot{x_6}$ are the angular accelerations $\ddot{q_1}, \ddot{q_2}, \ddot{q_3}$, respectively.

Also, the state space model can be given in terms of the velocities $\dot{q_3}$ and $\dot{q_2}$ as

$$\ddot{q_1} = \dot{q_3}M_1C_1' + M_1G_1 + \dot{q_3}M_2C_2' + M_2G_2 + \dot{q_2}M_3C_3' + M_3G_3 - M_1\tau_1 - M_2\tau_2 - M_3\tau_3 \tag{3.2.89}$$

$$\ddot{q_2} = \dot{q_3}M_2C_1' + M_2G_1 + \dot{q_3}M_4C_2' + M_4G_2 + \dot{q_2}M_5C_3' + M_5G_3 - M_2\tau_1 - M_4\tau_2 - M_5\tau_3 \tag{3.2.90}$$

$$\ddot{q_3} = \dot{q_3}M_3C_1' + M_3G_1 + \dot{q_3}M_5C_2' + M_5G_2 - \dot{q_2}M_6C_3' - M_6G_3 - M_3\tau_1 - M_5\tau_2 + M_6\tau_3 \tag{3.2.91}$$

$$\begin{bmatrix} \dot{x_1} \\ \dot{x_2} \\ \dot{x_3} \\ \dot{x_4} \\ \dot{x_5} \\ \dot{x} \end{bmatrix} = \begin{bmatrix} 0 & 1 & 0 & 0 & 0 & 0 \\ 0 & 0 & 0 & M_3C_3' & 0 & M_1C_1' + M_2C_2' \\ 0 & 0 & 0 & 1 & 0 & 0 \\ 0 & 0 & 0 & M_5C_3' & 0 & M_2C_1' + M_4C_2' + M_5C_3' \\ 0 & 0 & 0 & 0 & 0 & 1 \\ 0 & 0 & 0 & -M_6C_3' & 0 & M_3C_1' + M_5C_2' \end{bmatrix} \begin{bmatrix} x_1 \\ x_2 \\ x_3 \\ x_4 \\ x_5 \\ x_6 \end{bmatrix} + \begin{bmatrix} 0 & 0 & 0 \\ -M_1 & -M_2 & -M_3 \\ 0 & 0 & 0 \\ -M_2 & -M_4 & -M_5 \\ 0 & 0 & 0 \\ -M_3 & -M_5 & M_6 \end{bmatrix} \begin{bmatrix} u_1 \\ u_2 \\ u_3 \end{bmatrix} \tag{3.2.92}$$

Note: The dominator M_{d3} is the determiner of the inertia matrix (3.2.70). To guarantee that the inertia matrix is positive definite and its inverse is exists, the length and mass values of the three-link finger (index) should be selected carefully to satisfy the condition ($M_{d3} \neq 0$).

Chapter 4

Simulation and Embedded Real-Time Experiment Results

In this chapter, we illustrate the simulation results of the tracking problem for two-link (thumb) and three-link (index) fingers. The selected trajectories for the tracking problem are two different nonlinear functions. Moreover, embedded real-time experiments are developed and implemented using the SDRE technique to track the desired trajectories for the two-link (thumb) and three-link (index) fingers of the robotic hand.

4.1 Simulation Results

4.1.1 Two-link Finger (Thumb) Simulation Results

Consider the state space model of the two-link finger (thumb) (3.2.48) that was derived in **Chapter 3**. The matrices A, B and C of the dynamic are given:

$$A = \begin{bmatrix} 0 & 1 & 0 & 0 \\ 0 & M_3C_2' & 0 & -M_2C_1' \\ 0 & 0 & 0 & 1 \\ 0 & -M_1C_2' & 0 & M_3C_1' \end{bmatrix}, B = \begin{bmatrix} 0 & 0 \\ M_2 & -M_3 \\ 0 & 0 \\ -M_3 & M_1 \end{bmatrix}, C = \begin{bmatrix} 1 & 0 & 0 & 0 \\ 0 & 1 & 0 & 0 \\ 0 & 0 & 1 & 0 \\ 0 & 0 & 0 & 1 \end{bmatrix}$$

The selected parameters of the thumb for the simulation are given in Table 4.1

Table 4.1: Thumb Parameters

Parameters	Values
Length (L_1^t, L_2^t)	4, 4 (cm)
Mass (m_1^t, m_2^t)	43, 31 (g)
Inertia (I_{zz1}^t, I_{zz2}^t)	60.02, 43.27 (g.cm^2)

The error weighted matrix $Q(t)$, the control weighted matrix $R(t)$, and the cost functional matrix $F(t)$ are selected as the following:

$$Q = \begin{bmatrix} 10^{15} & 0 & 0 & 0 \\ 0 & 10^{10} & 0 & 0 \\ 0 & 0 & 10^{15} & 0 \\ 0 & 0 & 0 & 10^{10} \end{bmatrix}, R = \begin{bmatrix} 10^4 & 0 \\ 0 & 10^4 \end{bmatrix}, F = \begin{bmatrix} 1 & 0 & 0 & 0 \\ 0 & 1 & 0 & 0 \\ 0 & 0 & 1 & 0 \\ 0 & 0 & 0 & 1 \end{bmatrix}$$

The desired trajectories parameters are given in Table 4.2

Table 4.2: Desired Trajectories Parameters

Parameters	Values
Time (t_0, t_f)	0, 10 (sec)
Desired Initial Position of Both Links ($q_1^{t_0}$, $q_2^{t_0}$)	0, 0 (rad)
Desired final Position of Second Link($q_2^{t_f}$)	1 (rad)

The simulation is performed for 10 sec to track the trajectories $-0.048t^2 + 0.0058t^3$ and $sin(t)$. The corresponding angels of the thumb fingertip are shown in Figures 4.1 and 4.2.

Figures 4.1 and 4.2, illustrate the optimal tracking responses of the thumb using the SDRE technique to track cubic polynomial and sinusoidal trajectories. Figures 4.3 and 4.4 show the optimal tracking errors and final stage tracking errors of the thumb fingertip.

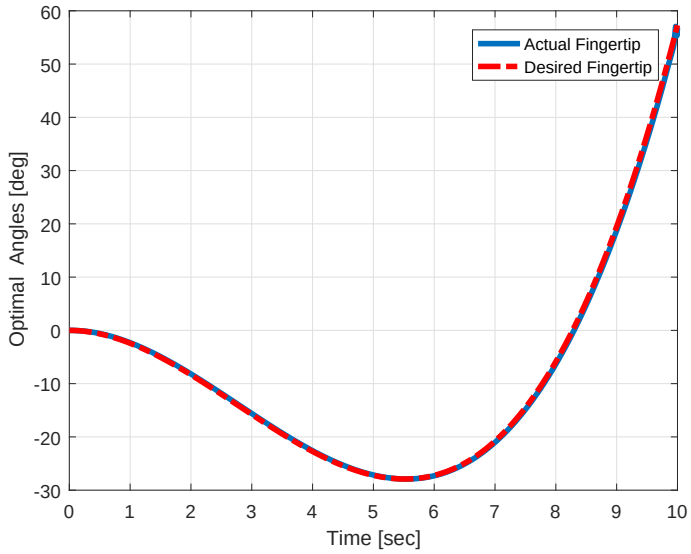

Figure 4.1: Desired and Actual Trajectories of the Thumb fingertip Tracking a Cubic Polynomial Function

4.1.2 Three-link Finger (Index) Simulation Results

Similarly, from (3.2.88) and (3.2.92), the matrices A, B and C of the index finger dynamic are given:

$$A = \begin{bmatrix} 0 & 1 & 0 & 0 & 0 & 0 \\ 0 & 0 & 0 & 0 & 0 & M_1C_1' + M_2C_2' + M_3C_3' \\ 0 & 0 & 0 & 1 & 0 & 0 \\ 0 & 0 & 0 & 0 & 0 & M_2C_1' + M_4C_2' + M_5C_3' \\ 0 & 0 & 0 & 0 & 0 & 1 \\ 0 & 0 & 0 & 0 & 0 & M_3C_1' + M_5C_2' - M_6C_3' \end{bmatrix} = \begin{bmatrix} 0 & 1 & 0 & 0 & 0 & 0 \\ 0 & 0 & 0 & M_3C_3' & 0 & M_1C_1' + M_2C_2' \\ 0 & 0 & 0 & 1 & 0 & 0 \\ 0 & 0 & 0 & M_5C_3' & 0 & M_2C_1' + M_4C_2' \\ 0 & 0 & 0 & 0 & 0 & 1 \\ 0 & 0 & 0 & -M_6C_3' & 0 & M_3C_1' + M_5C_2' \end{bmatrix}$$

$$B = \begin{bmatrix} 0 & 0 & 0 \\ -M_1 & -M_2 & -M_3 \\ 0 & 0 & 0 \\ -M_2 & -M_4 & -M_5 \\ 0 & 0 & 0 \\ -M_3 & -M_5 & M_6 \end{bmatrix}, C = \begin{bmatrix} 1 & 0 & 0 & 0 & 0 & 0 \\ 0 & 1 & 0 & 0 & 0 & 0 \\ 0 & 0 & 1 & 0 & 0 & 0 \\ 0 & 0 & 0 & 1 & 0 & 0 \\ 0 & 0 & 0 & 0 & 1 & 0 \\ 0 & 0 & 0 & 0 & 0 & 1 \end{bmatrix}$$

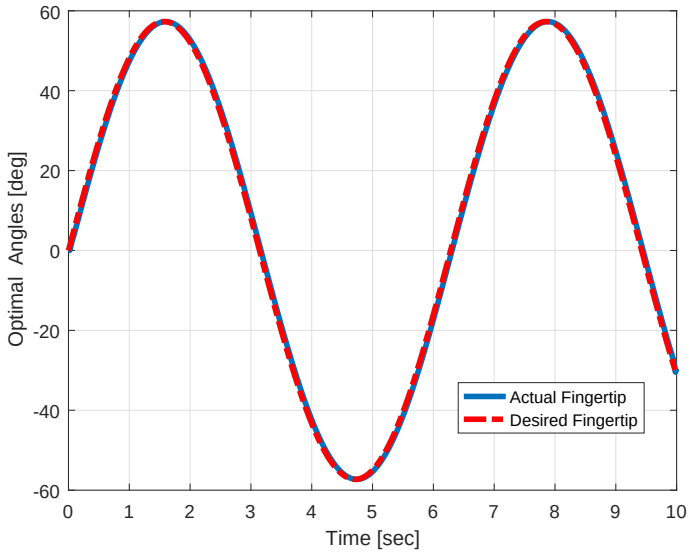

Figure 4.2: Desired and Actual Trajectories of the Thumb fingertip Tracking a Sinusoidal Function

The selected parameters of the Index for the simulation are given in Table 4.3

Table 4.3: Index Parameters

Parameters	Values
Length (L_1^t, L_2^t, L_3^t)	4, 4, 3 (cm)
Mass (m_1^t, m_2^t, m_3^t)	45, 25, 17 (g)
Inertia (I_{zz1}^t, I_{zz2}^t, I_{zz3}^t)	93.75, 33.33, 11.25 (g.cm^2)

The error weighted matrix $Q(t)$, the control weighted matrix $R(t)$, and the cost functional matrix $F(t)$ are selected as the following:

$$Q = \begin{bmatrix} .7 \times 10^8 & 0 & 0 & 0 & 0 & 0 \\ 0 & 7.7 \times 10^2 & 0 & 0 & 0 & 0 \\ 0 & 0 & .7 \times 10^8 & 0 & 0 & 0 \\ 0 & 0 & 0 & 7.7 \times 10^2 & 0 & 0 \\ 0 & 0 & 0 & 0 & .7 \times 10^8 & 0 \\ 0 & 0 & 0 & 0 & 0 & 7.7 \times 10^2 \end{bmatrix}$$

$$R = \begin{bmatrix} .2 \times 10^{-}2 & 0 & 0 \\ 0 & .2 \times 10^{-}2 & 0 \\ 0 & 0 & .2 \times 10^{-}2 \end{bmatrix}, C = \begin{bmatrix} 1 & 0 & 0 & 0 & 0 & 0 \\ 0 & 1 & 0 & 0 & 0 & 0 \\ 0 & 0 & 1 & 0 & 0 & 0 \\ 0 & 0 & 0 & 1 & 0 & 0 \\ 0 & 0 & 0 & 0 & 1 & 0 \\ 0 & 0 & 0 & 0 & 0 & 1 \end{bmatrix}$$

The desired trajectories parameters are given in Table 4.4

Table 4.4: Desired Trajectories Parameters

Parameters	Values
Time (t_0, t_f)	0, 10 (sec)
Desired Initial Position of Links ($q_1^{t_0}$, $q_2^{t_0}$, $q_3^{t_0}$)	0, 0, 0 (rad)
Desired Final Position of the Fingertip ($q_3^{t_f}$)	1 (rad)

Figures 4.5 and 4.6, illustrate the optimal tracking responses of the index finger using SDRE technique to track cubic polynomial and sinusoidal trajectories. The tracking errors and final stage tracking errors are shown in Figures 4.7 and 4.8.

4.2 Embedded Real-Time Experiment Results

For the purpose of real-time implementation, a graphical programming code is developed via LabVIEW©software to design a finite-time nonlinear closed-loop optimal tracking controller using the SDRE technique for the thumb and index finger. Moreover, the code is implemented using the MyRio module to track a sinusoidal trajectory and generate the optimal input signals for the servo motors that is used. We should note that each finger has only one Futaba micro servo motor (s3114).

4.2.1 Two-link Finger (Thumb) Experiment Results

In this section, we present the real-time experiment results of the SDRE technique for the thumb. The design of the block diagram and front panel for the SDRE

controller for the thumb are shown in Figures 4.9 and 4.10

The block diagram (Figure 4.9) contains a MathScript Node that has the thumb dynamic, desired trajectory (sinusoidal), and SDRE tracking controller. The PWM signals are generated by PWM module based on the optimal state values of the fingertip to drive the servo motor to the desired position. Also, the block diagram includes a main loop (while-loop) and a sub loop (for-loop) with a wait function. Moreover, the front panel (Figure 4.9) has two waveform charts to display the actual and desired trajectories and the tracking error, in addition to a numeric control to change the frequency of the servo motor.

4.2.2 Three-link Finger (Index) Experiment Results

Here, the block diagram and the front panel designs (Figures 4.11 and 4.12) of the SDRE tracking controller for the index finger are developed and implemented. Real-time experiment results are presented in Figure 4.12.

Figure 4.11 shows that the block diagram of the SDRE tracking controller of the index finger has the similar structure to the thumb controller. The main difference is the script that is used of the MathScript Node. Also, a display of the actual and desired trajectories and the tracking error in real-time are provided using waveform charts in the front panel (Figure 4.12).

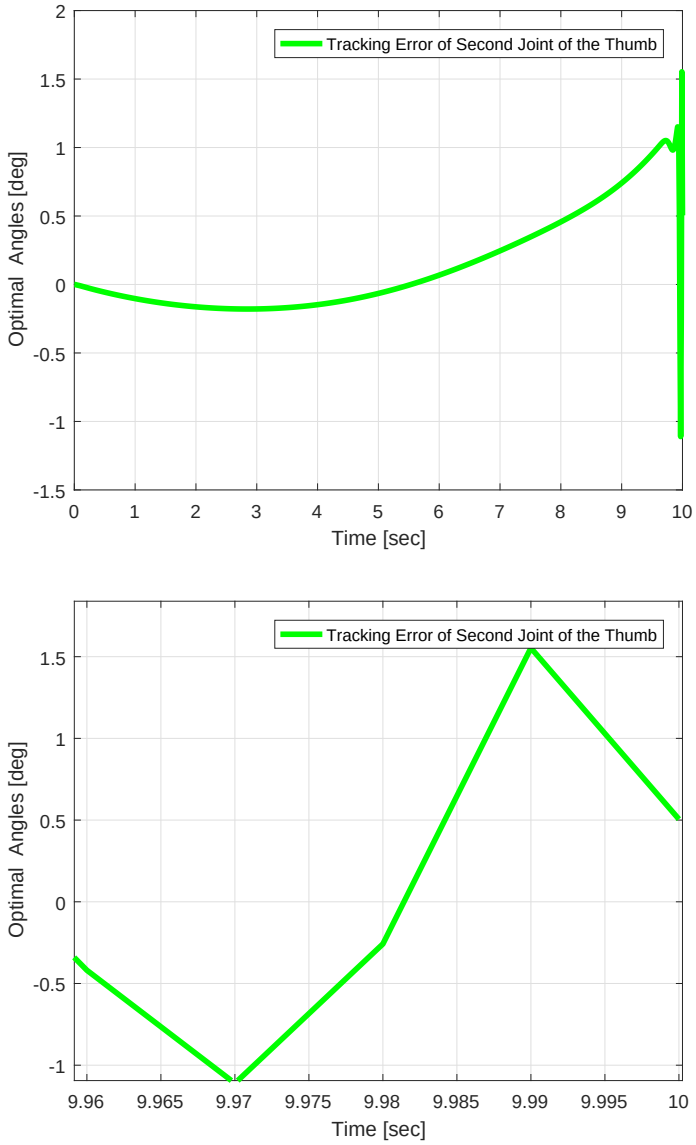

Figure 4.3: Tracking Error of the Thumb Fingertip tracking a Sinusoidal Function

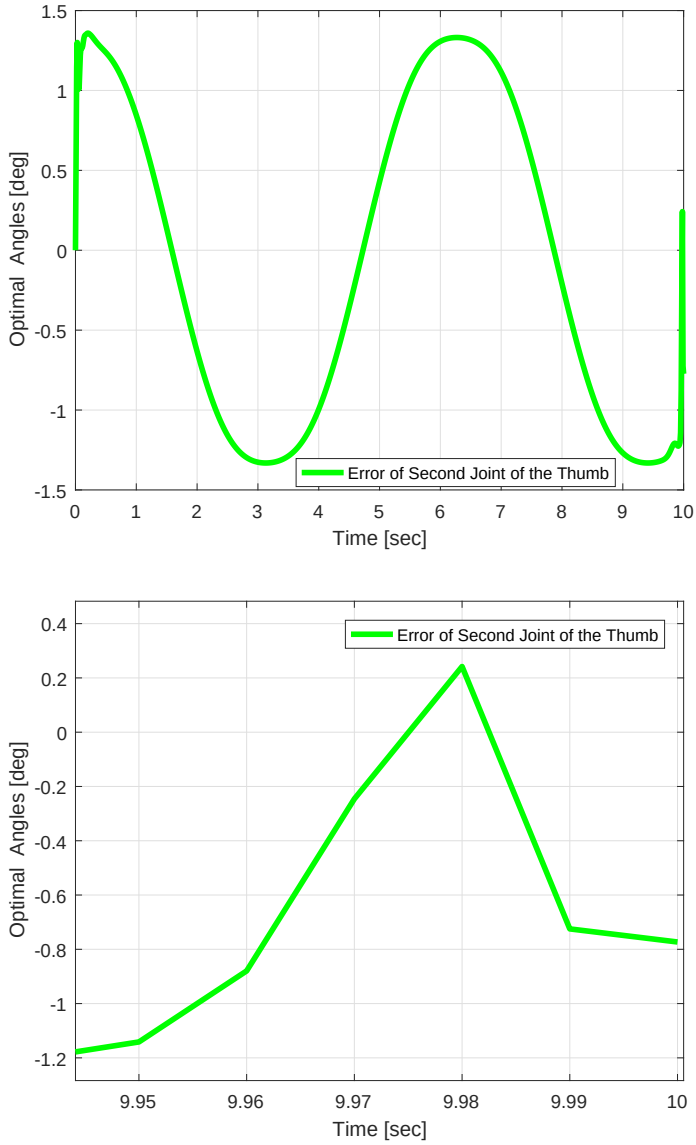

Figure 4.4: Tracking Error of the Thumb Fingertip tracking a Sinusoidal Function

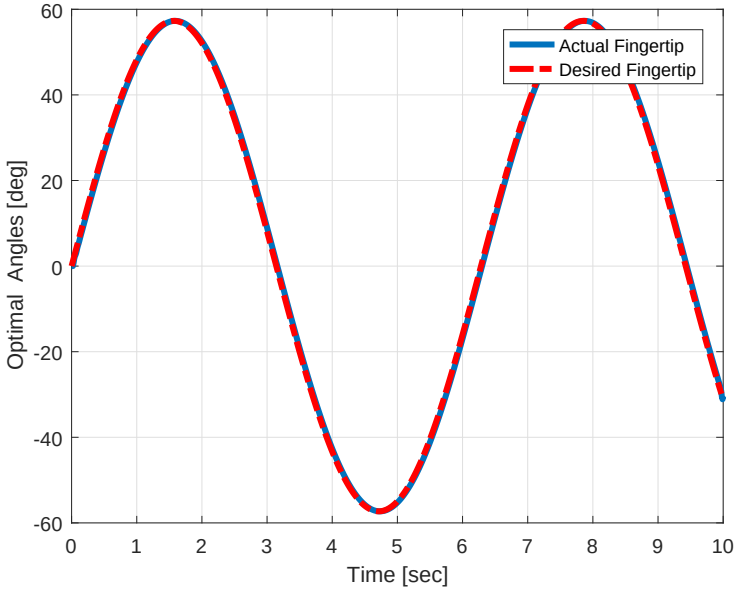

Figure 4.5: Desired and Actual Trajectories of the Index Finger Tracking a Sinusoidal Function

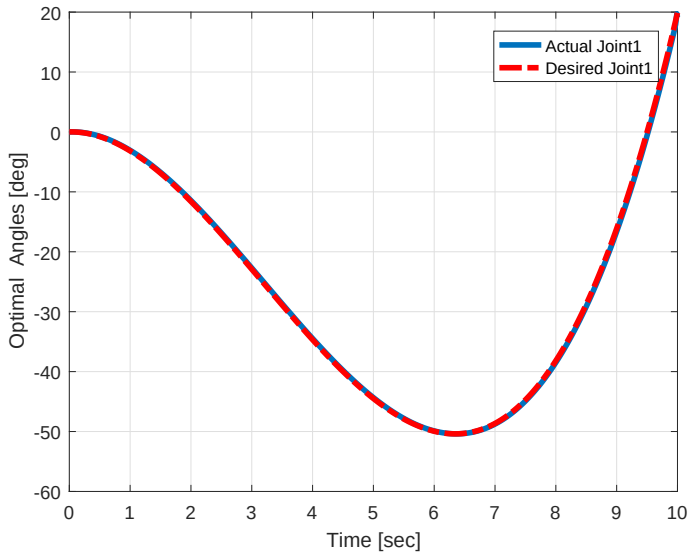

Figure 4.6: Desired and Actual Trajectories of the Index Finger Tracking a Cubic Polynomial Function

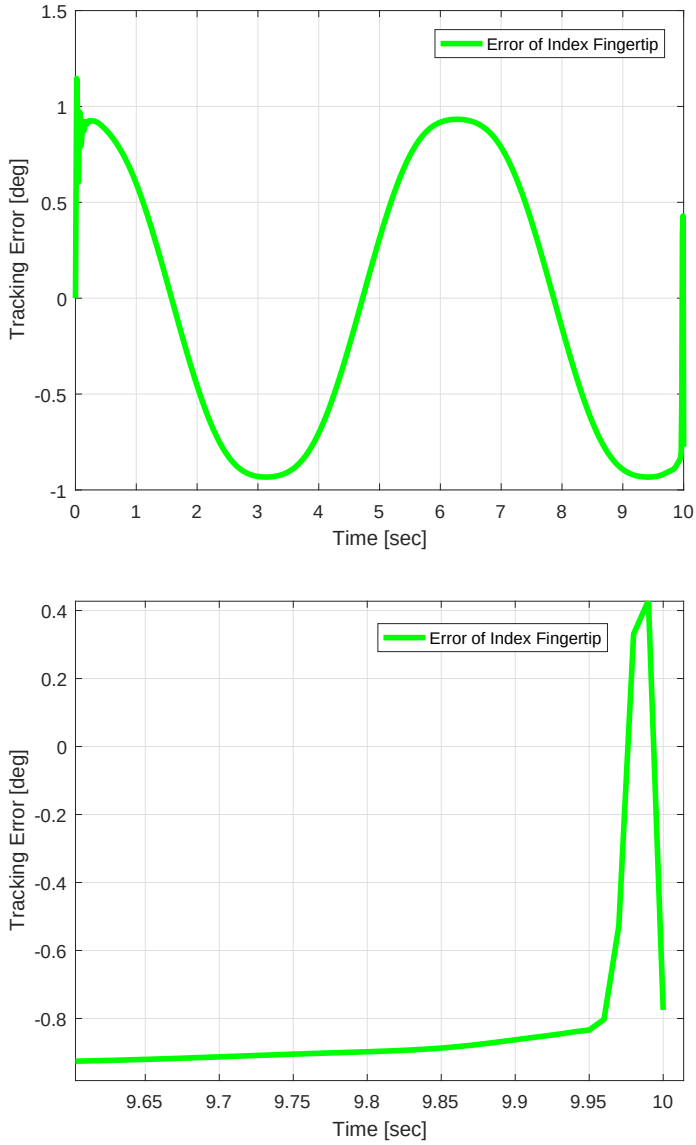

Figure 4.7: Tracking Error of Index fingertip Tracking a Sinusoidal Function

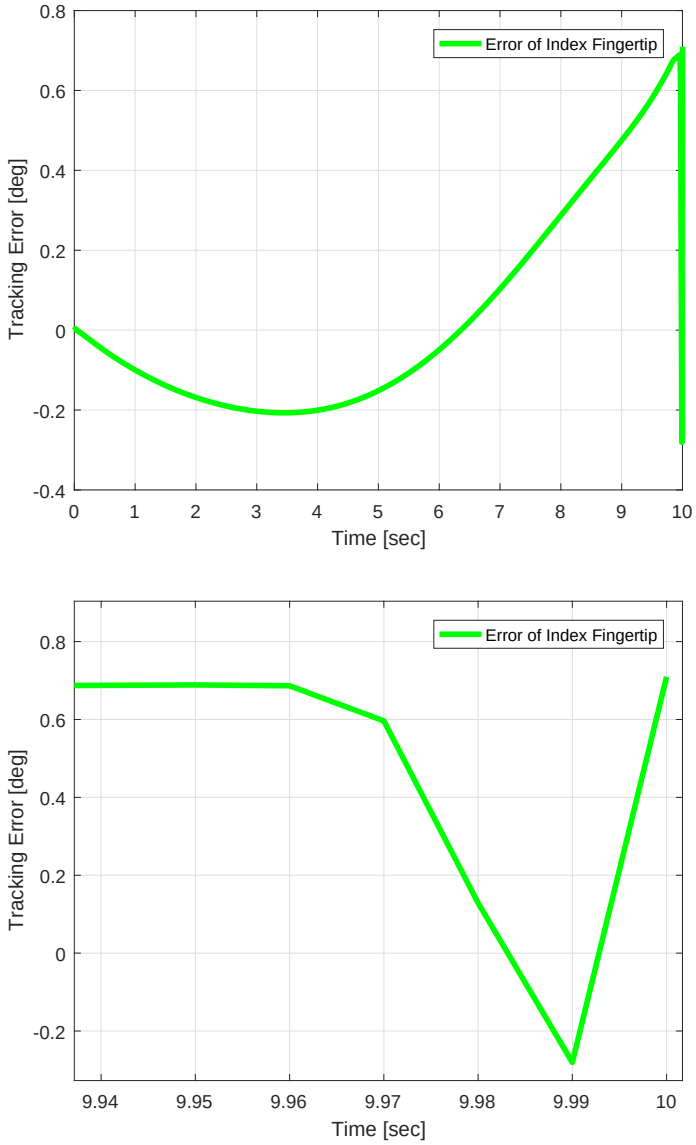

Figure 4.8: Tracking Error of Index fingertip Tracking a Cubic Polynomial Function

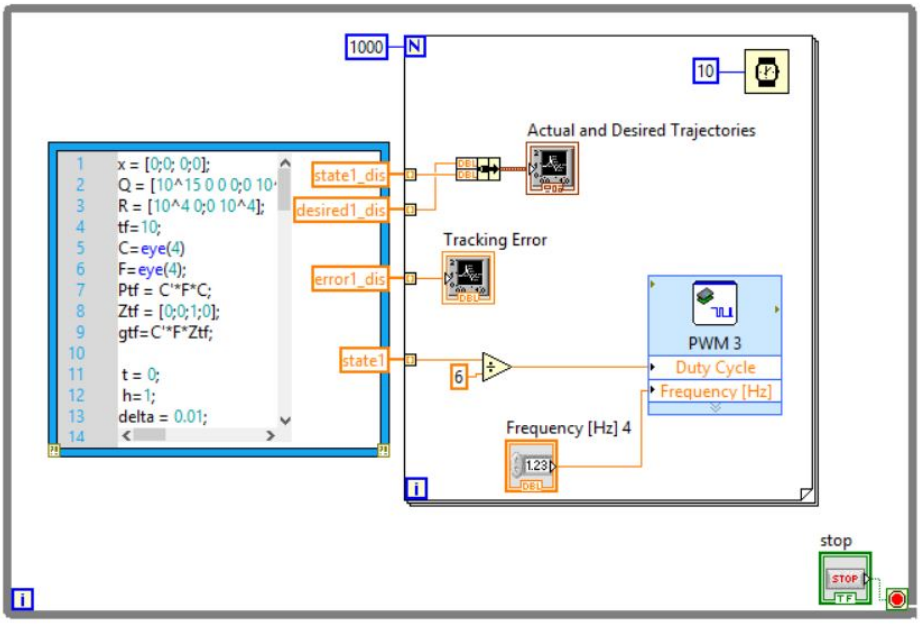

Figure 4.9: Labview Block Diagram Design for the SDRE Controller of the Thumb

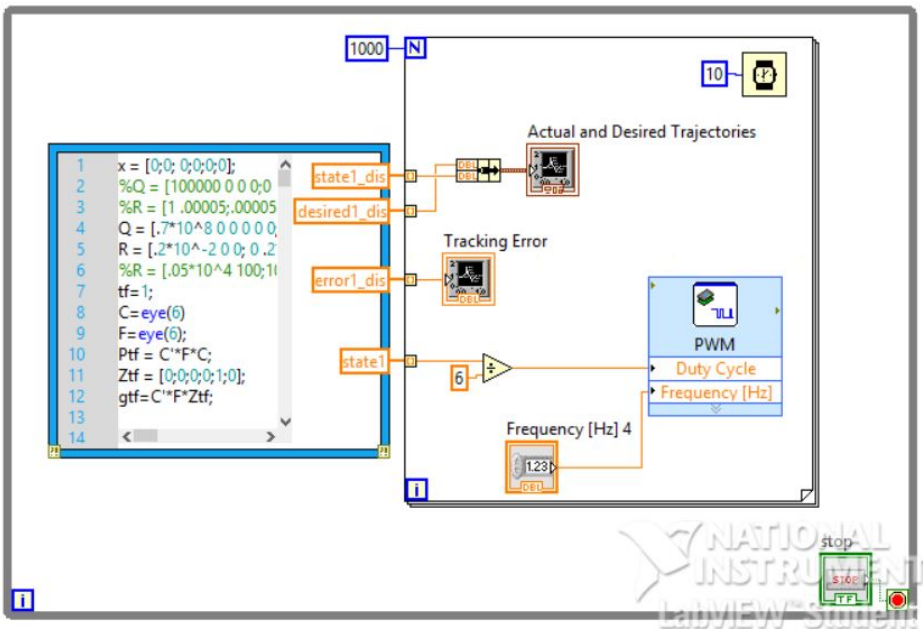

Figure 4.10: Labview Block Diagram Design for the SDRE Controller of the Index Finger

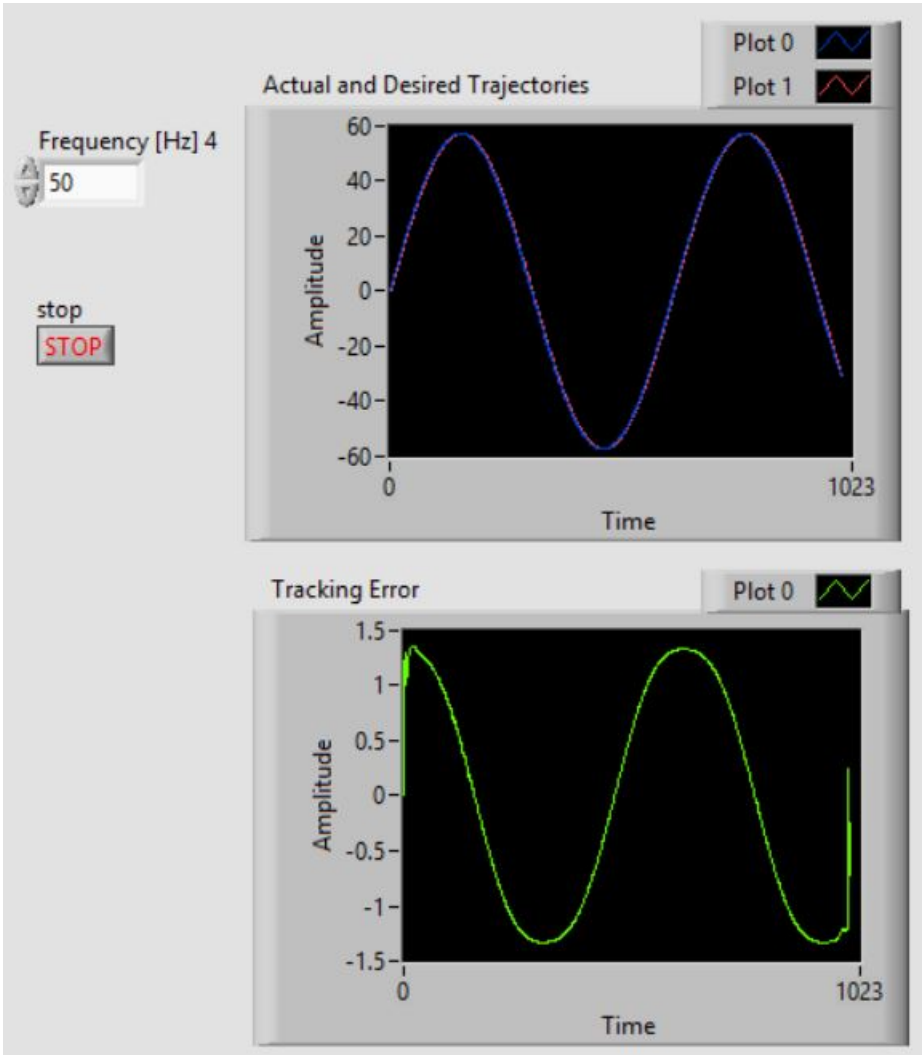

Figure 4.11: Labview Front Panel for the Controller of the Thumb

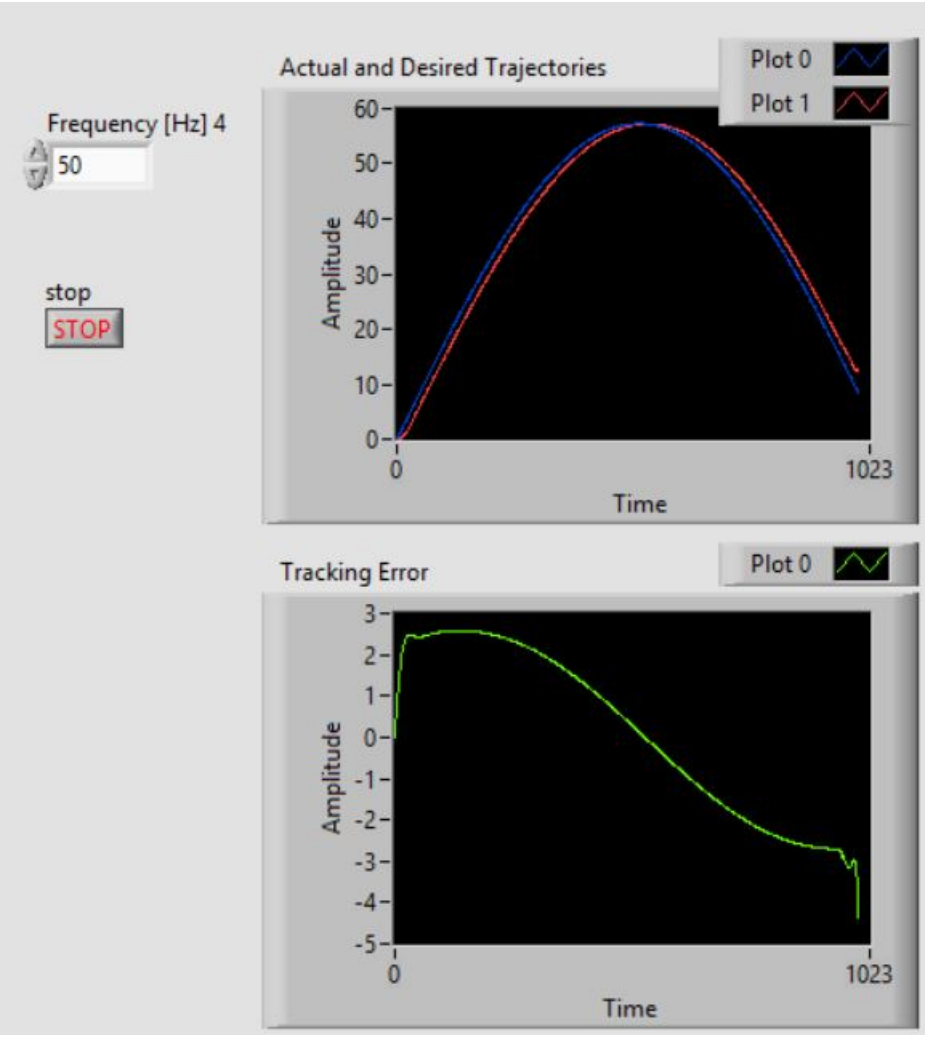

Figure 4.12: Labview Front Panel for the Index Finger

Chapter 5

Conclusion and Future Work

5.1 Discussion and Conclusion

In this research, a new mathematical representation of the dynamics of two-link (thumb) and three-link (index) fingers were presented in state space model. An online finite-time nonlinear optimal control tracking system using SDRE technique was applied to track nonlinear trajectories such as cubic polynomial and sinusoidal functions. Simulation results of two-link and three-link fingers were obtained and presented via MATLAB©. Embedded real-time experiments were developed for the two-link (thumb) and three-link (index) fingers via LabVIEW©and implemented using the MyRIO©module to track sinusoidal trajectories in real-time and generate the optimal PWM signals to drive the Futaba micro servo motor (s3114).

Simulation results of the thumb (Figures 4.1 and 4.2) show optimal tracking responses using the state dependent Riccati equation (SDRE) technique, tracking cubic polynomial and sinusoidal trajectories with minimum tracking error. The final stage tracking errors are 0.5^o and -0.8^o, Figures 4.3 and 4.4, respectively. Also, Figures 4.3 and 4.4 show that the change of the tracking error is nonlinear (unsteady) due to the difference of the dynamic nature between the robotic hand and the tracking trajectories; therefore, the variation $\mathbf{z}(t) - \mathbf{y}(t)$ is not constant. Also, the approach that is used to solve the differential Riccati equation (DRE) is an approximate solution that is based on calculating the steady state value $\mathbf{P_{ss}}(\mathbf{x})$.

Similarly, from Figures 4.5 and 4.6, it is obvious that the tracking responses of the index finger using the SDRE technique to track cubic polynomial and sinusoidal functions are optimal responses with minimum tracking errors and acceptable final stage tracking errors -0.8^o and 0.7^o, Figures 4.7 and 4.8, respectively. Also, Figures 4.7 and 4.8 show that the tracking errors are nonlinear (unsteady) due to the same two reasons that we discussed. First, the variation $\mathbf{z}(t) - \mathbf{y}(t)$ is not constant due to the nonlinearity of the dynamic and desired trajectories. The same approximate approach is used to solve the differential Riccati equation (DRE) by computing the steady state value $\mathbf{P_{ss}}(\mathbf{x})$.

Embedded real-time experiments were developed via LabVIEW©and implemented on MyRIO©to close the gap between simulation results and real-time applications.

The waveform charts in Figure 4.11 of the SDRE controller for the thumb are congruent with the simulation results. In other words, we successfully achieved an identical optimal tracking response and same tracking error in real-time.

Figure 4.12 show that the SDRE tracking controller for the index finger is still capable of tracking the desired trajectory in real-time but can not maintain the closed-loop error $e(t)$ closer to zero. That can be explained by the complexity of the index finger's dynamic and the approximate solution that is used in this technique.

In conclusion, the SDRE technique is ultimately effective in real-time experiments and maintains the same responses that is obtained in the simulations for less complex nonlinear state-dependent systems such as the two-link finger (thumb). On the other hand, the SDRE technique does not eliminate the closed-loop error and keep it closer to zero when it is applied to complex nonlinear state-dependent systems such as three-link finger (index) due to the approximate approach that is used to solve the differential Riccati equation (DRE).

5.2 Future Work

Since we successfully obtained the dynamics of the two-link and three-link fingers in a state space model, this research can be continued to accomplish the following goals:

1. Apply a nonlinear optimal tracking control techniques, without using linearization techniques, such as the SDRE technique for all other fingers.

2. Electromyography signals (EMGs) can be used to generate the desired trajectories to track the hand motion of a healthy hand instead of using nonlinear functions such as cubic polynomial and sinusoidal trajectories.

3. Develop a new tracking approach to solve the differential Riccati equation (DRE) forward in time using the methodology that was developed [21] for linear quadratic optimal control systems to solve the algebraic Riccati equation which MATLAB©does not have.

4. Implementing a nonlinear optimal tracking controller using the FPGA processor in the MyRIO©module so that the module does not need to be connected to LabVIEW©during real-time operations.

5. Finally, design a robotic/prosthetic hand using a 3D printer.

Bibliography

[1] A. Barraud. A new numerical solution of xdot=a1*x+x*a2+d, x(0)=c. *IEEE Transaction on Automatic Control*, 22(6):976–977, Dec. 1977.

[2] L. Birglen, T. Laliberte, and C. Gosselin. *Underactuated Robotic Hands*. Springer Tracts in Advanced Robotics. Springer-Verlag, Berlin, Germany, 2008.

[3] S. Bouchard. Robotic arms help upgrade international space station. Technical note, IEEE Spectrum, New York, NY, July 22 2009. (http://spectrum.ieee.org/automaton/robotics/humanoids).

[4] J.V. Breakwell, J.L. Speyer, and A.E. Bryson, Jr. Optimization and control of nonlinear systems using the second variation. *SIAM J. Control*, 1(2):193–223, 1963.

[5] B. Brumson. Chemical and hazardous material handling robotics. Technical note, Robotic Industries Association, Ann Arbor, MI, January 18 2007. (http://www.robotics.org).

[6] T. Çimen. State-dependent Riccati equation (SDRE) control: a survey. *Proceedings of the 17th World Congress of the International Federation of Automatic Control (IFAC), Seoul, Korea*, pages 6–11, 2008.

[7] T. Çimen. Development and validation of a mathematical model for control of constrained nonlinear oil tanker motion. *Mathematical and Computer Modeling of Dynamical Systems*, 15(1):1749, 2009.

[8] C.-H. Chen. *Hybrid Control Strategies for Smart Prosthetic Hand*. PhD thesis, Idaho State University, 2009.

[9] C.-H. Chen and D.S. Naidu. Hybrid control strategies for a five-finger robotic hand. *Biomedical Signal Processing and Control*, 8:168–174, July 2013.

[10] Chen-Hung Chen and D. Subbaram Naidu. *Fusion of Hard and Soft Control Strategies for the Robotic Hand*. IEEE, WILEY.

[11] J.R. Cloutier. State-dependent Riccati equation techniques: An overview. *Proc. American Control Conference*, 2:932–936, 1997.

[12] Z. Gajic and M. Qureshi. The Lyapunov matrix equation in system stability and control. *New York: Dover Publications*, 2008.

[13] A. Heydari and S.N. Balakrishnan. Path planning using a novel finite-horizon suboptimal controller. *Journal of Guidance, Control, and Dynamics*, pages 1–5, 2013.

[14] M. Jamshidi and P.J. Eicker, editors. *Robotics and remote systems for hazardous environments*. Prentice Hall PTR, Upper Saddle River, NJ, 1993.

[15] R. N. Jazar. *Theory of Applied Robotics. Kinematics, Dynamics, and Control*. Spring, New York, USA, 2007.

[16] D. G. Kamper, E. G. Cruz, and M. P. Siegel. Stereotypical fingertip trajectories during grasp. *J. Neurophysiol.*, 90:3702–3710, 2003.

[17] R. Kelly, V. Santibanez, and A. Loria. *Control of Robot Manipulators in Joint Space*. Springer, New York, USA, 2005.

[18] A. Khamis and D.S. Naidu. Nonlinear optimal tracking using finite-horizon state dependent Riccati equation (SDRE). In *Proceedings of the 4th International Conference on Circuits, Systems, Control, Signals (WSEAS)*, pages 37–42, August 2013. Valencia, Spain.

[19] G.L. Luo and G.N. Saridis. L-Q design of PID controllers for robotic hand. *IEEE Journal of Robotics and Automation*, RA-1(3):152–159, September 1985.

[20] X. Luo, T. Kline, H. C. Fisher, K. A. Stubblefield, R. V. Kenyon, and D. G. Kamper. Integration of augmented reality and assistive devices for post-stroke

hand opening rehabilitation. In *The International Conference of IEEE Engineering in Medicine and Biology Society*, Shanghai, China, 2005.

[21] D.S. Naidu. *Optimal Control Systems*. CRC Press, 2003.

[22] D.S. Naidu and V.K. Nandikolla. Fusion of hard and soft control strategies for left ventricular ejection dynamics arising in biomedicine. In *Proceedings of the Automatic Control Conference (ACC)*, pages 1575–1580, Portland, OR, June 8-10 2005.

[23] J. Nazarzadeh, M. Razzaghi, and K. Nikravesh. Solution of the matrix Riccati equation for the linear quadratic control problems. *Mathematical and Computer Modelling*, 27(7):51–55, 1998.

[24] H.M. Nguyen and D.S. Naidu. *IAENG Transactions on Engineering Technologies - Special Issue of the World Congress on Engineering and Computer Science 2012*, chapter Optimal Power Conversion for Standalone Wind Energy Conversion Systems using Fuzzy Adaptive Control. Springer-Verlag, Germany, 2013.

[25] T. Nguyen and Z. Gajic. Solving the matrix differential Riccati equation: a Lyapunov equation approach. *IEEE Trans. Automatic Control*, 55(1):191–194, 2010.

[26] What are the applications of an industrial robot arm? Website. http://www.robots.com.

[27] V. Salehi, S. Kahrobaee, and S. Afsharnia. Power flow control and power quality improvement of wind turbine using universal custom power conditioner. In *Industrial Electronics, 2006 IEEE International Symposium on*, volume 3, pages 1888 –1892, July 2006.

[28] B. Siciliano, L. Sciavicco, L. Villani, and G. Oriolo. *Robotics: Modelling, Planning and Control*. Springer-Verlag, London, UK, 2009.

[29] U.S. Food and Drug Administration, Silver Spring, MD. *Computer-Assisted Surgical Systems: Common uses of Robotically-Assisted Surgical (RAS) Devices*, March 11 2015.

[30] L. Vandenberghe, V. Balakrishnan, R. Wallin, A. Hansson, and T. Roh. *Positive Polynomials in Control*, volume 312, chapter Interior-point methods for semidefinite programming problems derived from the KYP lemma, pages 195–238. D. Henrion and A. Garulli, Eds. Berlin, Germany: Springer Verlag, 2005.

[31] L. Zollo, S. Roccella, E. Guglielmelli, M. C. Carrozza, and P. Dario. Biomechatronic design and control of an anthropomorphic artificial hand for prosthetic and robotic applications. *IEEE/ASME Transactions on Mechatronics*, 12(4):418–429, August 2007.